Bathymetry and Geomorphology of Shelikof Strait and the Western Gulf of Alaska

Mark Zimmermann [1,*] , **Megan M. Prescott** [2] **and Peter J. Haeussler** [3]

[1] National Marine Fisheries Service, Alaska Fisheries Science Center, National Oceanic and Atmospheric Administration (NOAA), Seattle, WA 98115, USA

[2] Lynker Technologies, Under contract to Alaska Fisheries Science Center, Seattle, WA 98115, USA; megan.prescott@noaa.gov

[3] U.S. Geological Survey, 4210 University Dr., Anchorage, AK 99058, USA; pheuslr@usgs.gov

* Correspondence: mark.zimmermann@noaa.gov; Tel.: +1-206-526-4119

Abstract: We defined the bathymetry of Shelikof Strait and the western Gulf of Alaska (WGOA) from the edges of the land masses down to about 7000 m deep in the Aleutian Trench. This map was produced by combining soundings from historical National Ocean Service (NOS) smooth sheets (2.7 million soundings); shallow multibeam and LIDAR (light detection and ranging) data sets from the NOS and others (subsampled to 2.6 million soundings); and deep multibeam (subsampled to 3.3 million soundings), single-beam, and underway files from fisheries research cruises (9.1 million soundings). These legacy smooth sheet data, some over a century old, were the best descriptor of much of the shallower and inshore areas, but they are superseded by the newer multibeam and LIDAR, where available. Much of the offshore area is only mapped by non-hydrographic single-beam and underway files. We combined these disparate data sets by proofing them against their source files, where possible, in an attempt to preserve seafloor features for research purposes. We also attempted to minimize bathymetric data errors so that they would not create artificial seafloor features that might impact such analyses. The main result of the bathymetry compilation is that we observe abundant features related to glaciation of the shelf of Alaska during the Last Glacial Maximum including abundant end moraines, some medial moraines, glacial lineations, eskers, iceberg ploughmarks, and two types of pockmarks. We developed an integrated onshore–offshore geomorphic map of the region that includes glacial flow directions, moraines, and iceberg ploughmarks to better define the form and flow of former ice masses.

Keywords: bathymetry compilation; Alaska Peninsula; Shelikof; Last Glacial Maximum; moraines; iceberg ploughmarks; glacial lineations; eskers; pockmarks

1. Introduction

Our bathymetry map of the western Gulf of Alaska (WGOA) extends along a 600 km-long portion of the continental shelf, ranging from Kodiak Island to the end of the Alaska Peninsula in Alaska, USA, at the northern edge of the North Pacific Ocean (Figure 1). The shelf in this part of the Gulf of Alaska (GOA) is about 200 km wide near Kodiak and narrows to about 100 km wide on the west end. The shelf contains numerous small islands and large (~100 km wide) offshore banks separated by significant depressions or troughs. Our map also includes the 50 km-wide and 200 km-long Shelikof Strait, which is located between the Kodiak Island archipelago and the Alaska Peninsula. Shelikof Trough begins in the area northwest of the Strait, turns more southerly at the west end of Kodiak, passes between the Semidi Islands and Chirikof Island, and reaches the edge of the shelf after another 250 km. Thus, at a total length of about 450 km, Shelikof Trough is the dominant feature of the shelf in the WGOA.

Erosion by ice sheets sculpted some of the seafloor features in the WGOA, including Shelikof Trough, but a detailed analysis of the distribution and geomorphology of the glacial landforms preserved on the seafloor has not been conducted owing to insufficient bathymetric detail. The aims of this project are to: (1) map broad-scale bathymetric features including troughs, banks and escarpments; (2) use this new bathymetry compilation to derive cross sections across Shelikof Strait, which will be useful for oceanographic and marine biological investigations; and (3) to map the distribution of subdued glacial landforms that are preserved on the seafloor.

Figure 1. Overview map of the western Gulf of Alaska study area. GEBCO (General Bathymetric Chart of the Oceans) bathymetry is shown for comparative purposes.

1.1. Exploration of the Western Gulf of Alaska and Shelikof Strait

European exploration of the WGOA dates to the 1700s, when notable seafarers such as Vitus Bering, James Cook, Grigory Shelikov, and George Vancouver began charting the area. In 1741, Bering, sailing on the *St. Peter*, encountered the Kodiak archipelago, Chirikof Island, the Alaska Peninsula, the Semidi Islands, and the Shumagin Islands while on his return voyage from charting the central GOA to Russia [1,2]. Bering was unable to distinguish Kodiak Island and the peninsula as separate entities, and his longitudes were in error. Alexsei Chirikof, his expedition second in command sailing on the *St. Paul*, missed all of the WGOA on his return voyage from charting some of the eastern GOA, except for briefly sighting the Kodiak archipelago [1,2]. Following the state-sponsored Bering and Chirikov expedition, more than 100 independent Russian fur-trading expeditions worked along the Aleutian Islands, slowly increasing cartographic knowledge of the island chain and some of the WGOA [3]. Notable expeditions include that of Stepan Glotov who over-wintered at Kodiak in 1763–1764, and that of Petr Krenitzin and Mikhail Levashov who produced a relatively complete and accurate map of the Aleutian Islands in 1768–1769 [3]. Captain Cook followed along the path of Bering as close as possible in 1778, recording more accurate latitude and longitude estimates for places that Bering

had charted, but he could not find Chirikof Island, and also did not discern that Kodiak Island and the Alaska Peninsula were separated by Shelikof Strait [4]. Cook was able to distinguish the Trinity Islands from Kodiak Island, but he mistakenly charted them as a single island [4]. Responding to the explorations of Cook and some state-sponsored Spanish expeditions to Alaska, in 1783 Grigory Shelikov led a three-vessel, state-sponsored expedition to Kodiak, establishing the first Russian colony there in 1784 [3]. He used the colony as a base for navigators Gerasim Izmailov and Demitri Bochorov to survey and chart the Kodiak archipelago, Shelikof Strait, the Alaska Peninsula, and other nearby waters. Captain George Vancouver charted the coast, islands and seafloor of the area in greater detail in 1794, most-notably determining the position of Chirikof Island [5,6]. Russia and several other nations continued the charting of Alaska in a competition for knowledge about her waterways and exploitable resources until the United States acquired Alaska from Russia in 1867. Jones [7] stated that these earlier surveys lacked sufficient detail and that the whole territory needed to be re-surveyed. The Aleutian Trench, which forms the southern border of this WGOA compilation, was not discovered until 1874, when the *Tuscarora* recorded some soundings exceeding 3000 fathoms (5487 m) while exploring for a shallow telegraph cable route across the North Pacific [8]. Professional U.S. hydrographic surveying of Alaska began in 1882 [7] and detailed paper maps termed "smooth sheets" were typically the final products of these surveys. A chart of the Alaska Peninsula from the U.S. Commission of Fish and Fisheries in 1888 (https://vilda.alaska.edu/digital/collection/cdmg11/id/17080/rec/81) shows the general shape of the Alaska Peninsula, most of the islands, Shelikof Strait, and two named banks, but omits the Aleutian Trench and has very few soundings throughout the entire area [9].

Presently the WGOA is well-charted for navigational purposes. The hydrographic "smooth sheet" surveys, conducted over the last century, provided the seafloor details for construction of the navigational charts. The navigational charts are often drawn at a relatively coarse resolution (~1; 100,000) in comparison to the smooth sheets (~1; 20,000) so much of the original information recorded on the smooth sheets is not generally available. Newer hydrographic surveys are generally conducted with multibeam sonars rather than the single-beam echosounders or lead-lines of the older smooth sheet surveys. Typically, this newer seafloor surveying technology results in the publication of continuous raster surfaces with cells only 4 or 5 m across, much more detailed than the historical smooth sheets, where lead-line or single-beam echosounder soundings were sometimes 100 m apart or more. While the smooth sheets and multibeam surveys are often excellent descriptors of the shallower, inshore seafloor areas, much of the offshore WGOA remains unsurveyed by these methods, so we sought alternative bathymetry data sources. Single-beam echosounder data or underway files from fisheries research cruises proved to be the best resource as bottom trawl surveys and midwater fish-acoustic surveys from the National Oceanic and Atmospheric Administration's (NOAA) Alaska Fisheries Science Center (AFSC) have crisscrossed this area with hundreds of thousands of kilometers of transects over the last few decades.

1.2. Bathymetry Compilations

This new WGOA compilation connects our previously published bathymetry surfaces of the Aleutian Islands [10] in the west, Cook Inlet [11] in the northeast, the Central Gulf of Alaska (CGOA) [12] in the east, and the eastern Bering Sea slope [13] in the northwest. All of these compilations used the same methods of proofing and editing the soundings against the original data sources—usually the smooth sheets—whenever possible. Thus, we are not using automated outlier detection analysis or smoothing to limit the impact of high and low bathymetric errors.

There have been several global and regional bathymetric compilations that included the WGOA, all utilizing different methods, but none of them checking for errors against the original smooth sheets. GEBCO (General Bathymetric Chart of the Oceans: https://www.gebco.net/) has been publishing global bathymetry charts for over a century, with the most recent available at a resolution of 30 arc-seconds (~926 m) [14] (Figure 1). Smith and Sandwell [15] developed an innovative method of calibrating satellite altimetry with vessel soundings and published their global map at a 2 arc-minute resolution

(~3704 m). Amante and Eakins [16] updated this calibrated satellite altimetry effort with a global map published at a resolution of 1 arc-minute resolution (~1852 m). Danielson et al. [17] utilized digitized U.S. and Russian navigational chart soundings, and other sources, to map the North Pacific Ocean and part of the Arctic Ocean. The Alaska Regional Office of the National Marine Fisheries Service (AKRO, Anchorage, AK, USA: https://alaskafisheries.noaa.gov/) has been producing bathymetry maps of Alaska (variable resolution, 2005; 40 m resolution, 2017).

1.3. Biological Research

The WGOA and Shelikof Strait provide important habitat for fish, birds, and marine mammals. An improved bathymetry map of the area will provide better descriptions of their habitat requirements. The largest Gulf of Alaska stock of walleye pollock (*Gadus chalcogrammus*) spawns in Shelikof Strait [18], and a new bathymetric map of the area may allow for better modeling of the oceanographic processes [19,20] that influence recruitment success. Smaller pollock stocks spawn in other areas of the WGOA, including Stepovak Bay and around the Shumagin Islands, Morzhovoi Bay and nearby Sanak Trough, and Pavlof Bay [18]. The National Marine Fisheries Service (NMFS) sablefish (*Anoplopoma fimbria*) longline survey [21] and the NMFS Gulf of Alaska bottom trawl survey have also indicated the unique importance of Shelikof Strait habitat to the documented population of sleeper sharks (*Somniosus pacificus*) seen there during surveys. We anticipate that our new WGOA bathymetry compilation will be useful for describing fish habitat because our previous bathymetry compilations were successfully utilized for modeled [22] essential fish habitat (EFH) descriptions for the Gulf of Alaska [23], the Aleutian Islands [24], and the eastern Bering Sea [25]. Digitizing smooth sheet shorelines and combining them with the smooth sheet soundings allowed shore-to-shore bathymetric descriptions of small study sites in the central Gulf of Alaska [26], the eastern Gulf of Alaska [27], and verification of smooth sheet data quality [28] for the Gulf of Alaska Integrated Ecosystem Research Project (GOA-IERP: https://www.nprb.org/gulf-of-alaska-project/about-the-project/). The GOA-IERP also produced maps of juvenile fish habitat [29], capelin (*Mallotus villosus*) habitat [30], and bathymetric steering of water currents in canyons [31] by using our improved CGOA bathymetry [12]. Detailed analysis of historical and recent smooth sheets from the Chignik area of the WGOA demonstrated significant inshore shallowing of some bays over a 70-year period, possibly due to redeposition of volcanic ash in eelgrass (*Zostera marina*) beds [32]. Coral and sponge habitats were also modeled using our improved bathymetry for the Aleutian Islands [33] and Gulf of Alaska [34].

1.4. Geological Setting

The southern Alaska margin has been a subduction zone for roughly the last 200 million years [35]. The Alaska Peninsula region contains classic features of a convergent margin, including a volcanic arc, a forearc high (Kodiak Island, Chirikof Island, the Shumagin Islands, Sanak Island), and the Aleutian Trench. Earthquakes define a Benioff zone that outlines the subducting Pacific plate, which moves at about 6 cm per year to the north–northwest in the study area. This region includes the area of a number of historical megathrust earthquake ruptures including the southwestern extent of the M9.2 1964 rupture—the second largest earthquake ever recorded.

The landscape of this region has been sculpted by multiple glaciations [36–38]. Retreat of ice from Sanak Island in the western part of the study area (Figure 1) occurred just prior to 17,000 yr B.P. and a terrestrial landscape had established itself on the island by about 16,300 yr B.P. [39]. At the northeastern end of the study area, Mann and Peteet [40] obtained a younger post-glacial radiocarbon age on peats of 14,700 yr B.P. Briner et al. [41] give a general discussion of deglaciation in Alaska. Prior work on the Alaska Peninsula outlines a series of glacial sequences [40,42–45]. Numerous glacial troughs incise the landscape, both above and below present sea level. The largest of these lies beneath Shelikof Strait. A principal finding of our present work is the abundance of glacial features that are preserved on the sea bottom, and we attempt to provide a synoptic view of the subaerial and submarine glacial features, without regard to the present shoreline.

Our new bathymetric database enables, for the first time, the former ice positions to be mapped from geomorphological observations of the WGOA region. Kaufman et al. [46] revised Kaufman and Manley [38] and interpreted the maximum limits of Pleistocene glaciers and late Wisconsinan glaciers across Alaska. Here, we use the more commonly used term of Last Glacial Maximum, or LGM, for this time period, which is inferred to be the position of glaciers from 26–19 kya [47]. (Note that Kaufman et al. [46] made no changes to the offshore Alaska Peninsula region from Kaufman and Manley [38], and all discussion of this region is in the older paper.) Kaufman and Manley [38] admit that many of their offshore limits are speculation. They relied heavily on Mann and Peteet [40] for their map of LGM limits of glaciers within the western Gulf of Alaska study area. They inferred that glaciers extended to the outer continental shelf and that ice terminated in a 50 m-tall ice cliff. We surmise their position of the LGM ice extent roughly follows the 120 m depth contour, but extends across deeper troughs, such as Shelikof Strait. There is a need to map LGM ice extents based on geomorphic observations, rather than inference.

2. Materials and Methods

2.1. Bathymetry Data Sources

We combined data from multiple bathymetry survey types to cover as much of the WGOA area as possible (Figure 2), as in our previous compilations (Table 1) [10–13,48]. The lack of the higher quality multibeam and smooth sheet data left much of the WGOA unmapped, so we utilized AFSC fisheries research cruise underway and echosounder files to fill in the gaps, where possible. This methodology was most similar to our eastern Bering Sea compilation [13], which still lacked much coverage of deeper waters. In the WGOA, some of the deeper Aleutian Trench area was mapped by the Scripps Institution of Oceanography on the R/V *Thomas Washington*, the GLORIA (Geological Long Range Inclined Asdic) project (https://coastalmap.marine.usgs.gov/gloria/) on the R/V *Farnella*, the Japan Agency for Marine-Earth Science and Technology (JAMSTEC) on the R/V *Mirai*, and the GEOMAR (Research Center for Marine Geophysics) Helmholtz Center for Ocean Research Kiel on the R/V *Sonne*.

2.1.1. Smooth Sheets

Smooth sheet surveys, conducted with sounding equipment ranging from lead-lines to single-beam echosounders, and with navigational methods ranging from visual shore station fixes and dead reckoning to GPS (Global Positioning System), covered much of the inshore area along the western part of the Alaska Peninsula, the central part of the peninsula, and within Shelikof Strait (Table 1). All of the smooth sheets from the western part of the peninsula (563,000 soundings) were from 1954 and older, with some dating back to 1913. All of the smooth sheets from the central peninsula (1,384,000 soundings) were from 1982 and newer, with the exception of a single survey from 1925 that accounted from <1% of soundings. Smooth sheets within Shelikof Strait (475,000 soundings) were a mix of older and newer smooth sheets, with about 44% of soundings being recorded prior to 1950. We also included some smooth sheets from the overlapping bathymetry compilations of the Aleutian Islands (72,000 soundings), Cook Inlet (33,000 soundings) and central Gulf of Alaska (125,000 soundings) for better continuity with previously published bathymetry surfaces. Many of these soundings are rounded to the nearest fathom (1.829 m), creating some vertical uncertainty, but the greatest errors are most likely horizontal errors from attempting to navigate too far offshore, and away from the visually observed shore stations.

2.1.2. Multibeam Surveys

Newer charting surveys were generally conducted with multibeam echosounders and GPS navigation. Some of these shallower surveys were conducted with aircraft using LIDAR (light detection and ranging) due to hazardous navigation for hydrographic vessels. Their survey products of bathymetry rasters were available at a wide variety of different horizontal resolutions, so we developed

methods of organizing them while grouping them together into a single, lower-resolution surface. We grouped individual multibeam surveys together at their native and coarsest resolution, unless such a surface was already available at NGDC (National Geophysical Data Center). For example, a multibeam survey might have a surface available at 1 m horizontal resolution only for the shallowest depths, at 2 m horizontal resolution only for middle depths, and at 4 m horizontal resolution only for the deepest depths. These would be combined together by using the "Resample" tool with "Bilinear" option to coarsen the 1 and 2 m surfaces to 4 m, and then by using the "Mosaic to new raster" tool in ArcMap (v.10.2.2, ESRI: Environmental Systems Research Institute, Redlands, CA) with the "Mosaic operator" option set as "Blend" to produce a 4 m horizontal resolution surface that covered the full extent of that multibeam survey. Often such a coarser comprehensive surface was already available at NGDC. Then all of the 4 m horizontal resolution surfaces in the same area would be combined by using the "Mosaic to new raster" tool, and the same would be done for multibeam surveys conducted at different horizontal resolutions, such as 5 m, 10 m, or 20 m. These interim products—larger than the individual multibeam surveys but of coarser resolution—were used for additional insight in the geological analysis. Each of these larger multibeam surfaces would then be reduced in resolution to 100 m by using the "Resample" function in ArcMap. Finally, all of the reduced-resolution 100 m surfaces would be combined into a regional 100 m surface by using the "Mosaic to new raster" tool. We repeatedly used this two-step process of "Resample" and "Mosaic to new raster" to produce the reduced-resolution surfaces around Chirikof Island, the Semidi Islands, the Shumagin Islands, and the Pavlof Islands because combining surfaces of different resolutions in a single step produced artifacts that could be misinterpreted as fish habitats or geological features. Vertical errors in multibeam depths were most likely minimized by subsampling and generalizing these data sets into coarser resolutions.

Previously unprocessed multibeam surveys, H11463-65 (Figure 3), were acquired from NOAA's NGDC Corresponding tide, sound velocity, and vessel files had to be created or reformatted from the raw data and the notes available in the Data Acquisition and Processing Report (DAPR). Tide station information was listed in the survey DAPR files and the corresponding data were downloaded from the NOAA Tides and Currents website. Once these files were properly formatted the multibeam data could be read, processed and edited in CARIS HIPS and SIPS (Computer Aided Resource Information System, Hydrographic Information Processing System and Sonar Information Processing System; version 7.1). The DAPR files contained detailed flowcharts for processing methods, combined with information contained in the field procedures manual obtained from the Office of Coast Survey (OCS: https://nauticalcharts.noaa.gov/) we copied OCS methods, to the best of our ability, for comparable work. BASE (Bathymetry Associated with Statistical Error) surfaces were created in CARIS at varying resolutions following guidelines found in the DAPR as well as resolution guidelines outlined in an OCS technical paper: U.S. Office of Coast Survey's Re-Engineered Process for Application of Hydrographic Survey Data to NOAA Charts [49]. The bathymetric data were then exported as ASCII files with Easting, Northing, and Depth attributes which were brought into ArcMap and converted into raster format.

Other smaller multibeam surveys were available from Uyak Bay on Kodiak Island (NOS: H10966), along the shelf edge west of Chirikof Island (Alaska Deep Sea Coral Initiative), and large, deepwater surveys of the Aleutian Trench were available from the R/V *Thomas Washington* 1984 MARATHON cruise (Scripps), MR01-K04 and MR99-K05 R/V *Mirai* cruises from JAMSTEC, and SO-96-1, SO-96-2, SO-97-1, SO-110-1B, and SO-110-2 cruises from the R/V *Sonne* (GEOMAR). From examining and editing these files, it appears that the greatest vertical errors for these deepwater soundings occurred when the vessel stopped and rotated in place for collecting a sample or changed course.
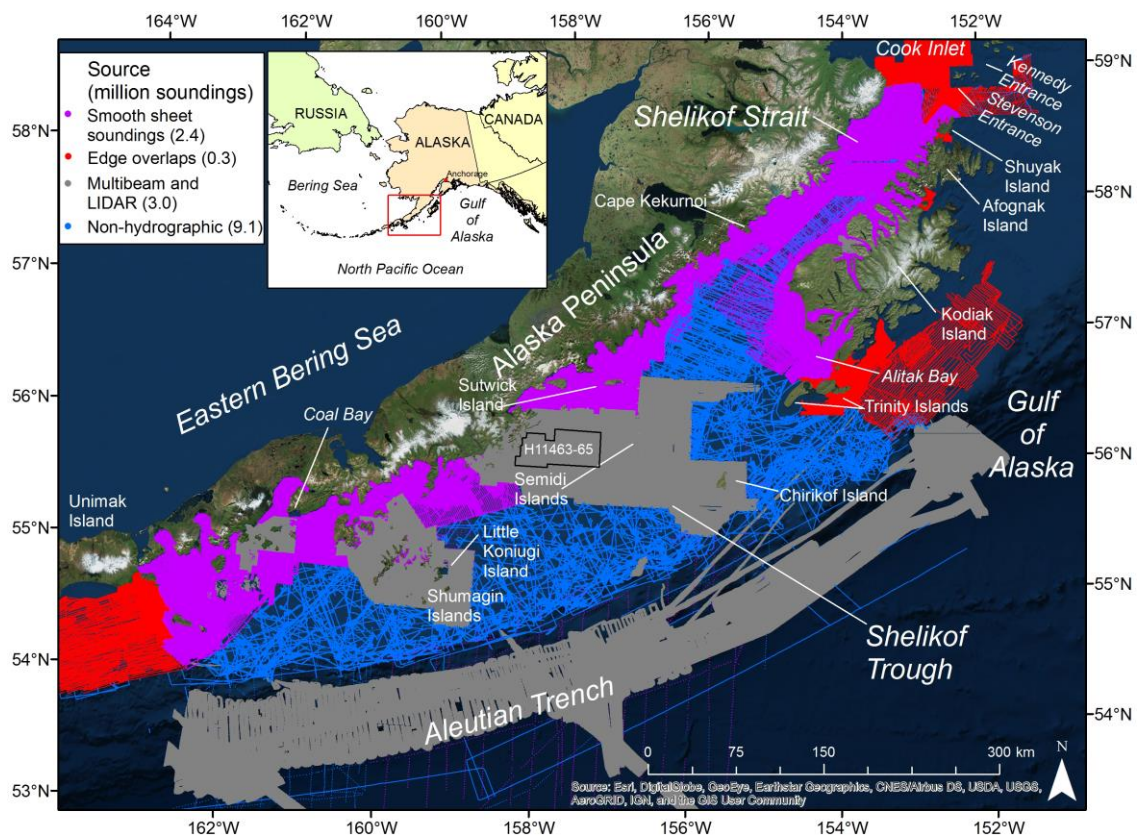
Figure 2. Sources of bathymetry data used in this western Gulf of Alaska compilation. Edge overlaps are repeated data sets from previously published bathymetry maps bordering this area. Non-hydrographic surveys are non-calibrated singlebeam surveys.

2.1.3. Singlebeam Surveys

We were initially reluctant to include singlebeam echosounder or underway files from AFSC bottom trawl and fish acoustic research cruises in our bathymetric compilation because these data sets were never collected for, nor calibrated for, producing bathymetric surfaces. For example, none of these cruises utilized bar checks, heave corrections, or speed-of-sound or tidal corrections—all key methods for ensuring proper representation of seafloor features. Unfortunately, much of the offshore WGOA has not been formally surveyed at a resolution sufficient for producing fish habitat or geological maps. In addition, there are some notable shallow "blank" areas on the map due to the absence of smooth sheet surveys, such as parts of the Sandman Reefs, Coal Bay outside of Pavlof Bay, the northwest side of Little Koniugi Island in the Shumagins, and areas around the Trinity Islands (Figure 3). However, an analysis comparing older and newer smooth-sheet bathymetry to recent fish acoustic research cruise-derived depths produced favorable results [28], so we began including some of these fishery cruises in our compilation iterations. Initial results indicated that these singlebeam cruises were at least partially successful in continuing seafloor features, such as banks, farther offshore from areas covered by smooth sheets and multibeam surveys. As we added more singlebeam cruises we found that there were some positive qualities of this type of data. AFSC fisheries acoustics cruises tend to collect echosounder data in long, uninterrupted transects across the shelf, minimizing depth detection errors often encountered during sharp turns. These acoustic cruises often routinely record the depth of their retractable echosounder, so that the depth below the sea surface is accounted for in their depth estimates. Echosounder and underway files from AFSC bottom trawl cruises have none of these fish acoustic cruise advantages, as long, straight transects are rare, sharp turns and changes in speed are common, and there is no accounting for depth below the sea surface of the echosounder. However, as we worked with more data from these cruises, we also realized that the bottom trawl

and acoustic cruises often crossed each other, allowing for some error-checking against extreme depth values. Eventually we included 18 bottom trawl cruises, 18 fish acoustic cruises, and two older cruises, proofing and editing them by inspection as we produced new bathymetry surfaces in an iterative process. The greatest vertical uncertainties for singlebeam surveys is unknown because they were uncalibrated, but most likely caused by hull depth estimation errors and mistaking a mid-water scattering layer for the seafloor.

Table 1. Summary of data sources used for this compilation. For continuity, we included small overlapping data sets from previously published compilations of the Aleutian Islands (AI edge), Cook Inlet (CI edge), and central Gulf of Alaska (CGOA edge). Large groups of overlapping smooth sheets covered much of the inshore area of the Western Peninsula, Central Peninsula, and Shelikof Strait, and there were just two offshore, deeper smooth sheets. Shallow multibeam data overlapped some of the shallow areas with smooth sheets, while deeper multibeam mostly covered the Aleutian Trench. Non-hydrographic quality single-beam data, mostly from fishery research cruises, filled a large gap in the outer shelf.

Type	Area	Year Start	Year End	Number of Cruises	Soundings (n)
Smooth sheets	AI edge	1936	1938	7	72,000
	CI edge	1965	1983	4	33,000
	CGOA edge	1907	1981	14	125,000
	Western Peninsula	1913	1954	82	563,000
	Central Peninsula	1925	1997	73	1,384,000
	Shelikof Strait	1906	2000	88	475,000
	Offshore (Deep)	1961	1961	2	1000
Multibeam	Onshore (Shallow)	2001	2015	158	2,599,000
	Offshore (Deep)	1984	2009	9	3,348,000
Non-hydrographic	Outer Shelf	1976	2017	40	9,113,000
All types	All areas	1907	2017	477	17,713,000

2.2. Bathymetry Raster Creation

The individual soundings from the smooth sheets, along with points derived from the lower resolution (100 m) multibeam surfaces and the soundings from the AFSC fish research acoustic and bottom trawl survey cruises were converted into a TIN (triangulated irregular network). The TIN produces a stiff surface with linear interpolation between points, such that there are no concave or convex interpolations between the input points. The TIN was displayed as a slope surface and steep areas were used as a guide to investigate potential errors in the various input sounding files. Where possible, the questionable digitized soundings were compared against their source files to identify and correct errors. As errors were corrected in the soundings files, new versions of the TIN were plotted and investigated in an iterative process. Eventually the corrected TIN was converted into a 100 m-resolution grid using the ArcMap function of "Conversion" within the 3D Analyst Tools, with the "Natural neighbors" option, to minimize and smooth interpolation artifacts. Areas of land were excised from the raster by comparing the raster points to a coast file (Alaska Department of Natural Resources).

2.3. Cross-Sections

We calculated the minimal cross-sectional areas across passes in the Shelikof Strait area by using the Interpolate Line feature of 3D Analyst of ArcMap so that we could define how the bathymetry influences oceanographic currents. Having the locations of minimum and maximum openings is important for oceanographic instrument placement and current flow estimates. To do this we drew cross-sections as straight lines between the tips of capes, points, heads and other unnamed locations that represented the shortest distances across the strait, between the Kodiak archipelago and the peninsula, and also within the passes of the Kodiak archipelago. If islands or rocks were intercepted

by the cross-section line, we made a line vertex at the high point and afterward we continued the line in a different direction, following the shortest distance from the high point to the mainland shoreline. This method utilizes the interpolated depth grid and not the individual soundings that were used to create the depth grid. Only zero or positive depths were used such that this interpolation was referenced to the vertical datum of MLLW (mean lower low water).

2.4. Submarine Geomorphology

We mapped the submarine geomorphology using the best bathymetry images available. In general, the multibeam data provided superior datasets and anchor our interpretations. Fine-scale features are not visible in regions with only single-beam bathymetry, and only glacial troughs and some moraine crests are observable from the single-beam data. We did not map features on the continental slope from the shelf break to the Aleutian Trench (Figure 1), and thus limit our interpretations to depths shallower than about 250 m. The linear nature of singlebeam data, even if collected at short time intervals, does not come close to approximating the resolution of multibeam data.

2.5. Subaerial Geomorphology

Given the abundance of submarine glacial features observed, we inferred that a better understanding of the offshore glacial geomorphology would come from combining the offshore map with the terrestrial record. Therefore, we mapped moraine crests and glacier flow directions for the Alaska Peninsula. We used the previously published geologic maps of Detterman et al. [42,43] and Wilson et al. [44,45] which cover the Cold Bay, False Pass, Port Moller, Stepovak Bay, Simeonof, Chignik, Sutwik, Ugashik, Bristol Bay, and Sutwik Island 250,000-scale quadrangles. As mentioned above, most terrestrial geologic maps of glacial features map the limit of morainal features. To keep our terrestrial map consistent with the submarine geomorphic map, we mapped either the crests of mapped moraines from their topographic expression, or the middle position of an arcuate morainal deposit, if the feature was more subtly expressed. For glacier flow directions, we utilized the downslope direction of U-shaped troughs that were clearly carved by glaciers. For troughs with abundant recent volcanic input, we did not map glacier flow directions.
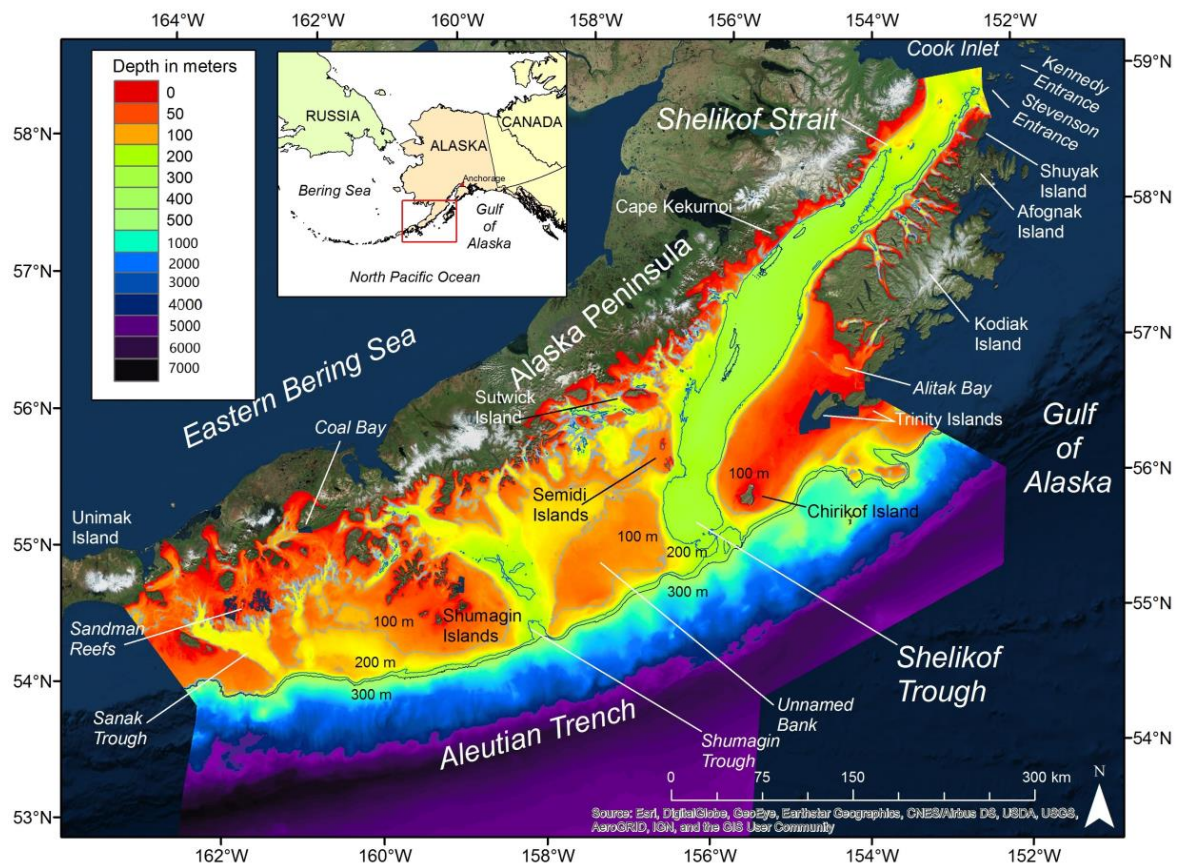
Figure 3. Bathymetry of the western Gulf of Alaska.

3. Results

3.1. Western Gulf of Alaska Bathymetry

We proofed, edited and digitized 17.7 million soundings from nearly 500 individual smooth sheets, multibeam/LIDAR surveys, and underway files for constructing a 100 m resolution grid or raster surface covering 220,000 km^2 of the WGOA (Figure 3). Altogether, the various sources provided at least one sounding for 32.9% of the 100 m grid cells, meaning that construction of the interpolated depth surface involved estimating depths for the remaining 67.1% of the grid cells. Smooth sheet soundings accounted for 15.0% of the soundings utilized (for smooth sheet data editing methods see [50]), while subsampled multibeam and LIDAR soundings (reduced to 100 m horizontal resolution) constituted 33.6% of the soundings (Table 1, Figure 2). Non-hydrographic quality data, mostly from vessel underway files, were the largest data source (51.4%), and covered much of the offshore area (Figure 2). Underway file resolution varied from one sounding per second to one sounding per several minutes. Despite our efforts to include new sources of bathymetry, the unsurveyed areas of the Sandman Reefs, Coal Bay, the northwest side of Little Koniugi Island, and the Trinity Islands are still blank.

3.2. Western Gulf of Alaska Cross Sections

The minimal areal opening of the Shelikof Strait (6.5 km^2) occurs at the northeast opening of the strait, between an unnamed location near Wonder Bay on Shuyak Island and Cape Douglas on the Alaska Peninsula (Table 2: Figure 4). While this is not the shortest distance across the strait, it is one of the shallowest (mean depth 141.5 m), and that is why this location represents the minimum cross-section. This minimal cross-section shows the deeper troughs along both sides of Shelikof Strait and intersects the northern-most escarpment. South of the northeast entrance to the strait, the

cross-sectional area gradually peaks at 8.9 km^2 between Cape Raspberry and Cape Ugyak. About 25 to 30 km south of the greatest minimum areal opening are the shortest cross-sectional openings across the strait, between Cape Ugat on Kodiak Island and Capes Kuliak (36.4 km) and Atushagvik (36.3 km) on the peninsula. While these shortest cross-sections still have larger areal openings than at the northeast entrance to the strait because the mean depth across the strait has increased to about 200 m, both are roughly equal-sized secondary minimal cross-sectional openings across the strait of about 7.3 km^2. This second minimum is near the area of maximum sediment deposition within Shelikof Strait [51]. South of Cape Ugat the cross-sectional openings increase steadily, exceeding 10 km^2, just prior to Cape Kekurnoi, which has the deepest average depth (218.5 m) of all cross-sections (not shown). South of Kekurnoi the cross-sectional areas continue increasing and the final cross-section, between Capes Ikolik and Igvak, at the western entrance to the strait, is more than double (15.0 km^2) the size of the eastern entrance to the strait.

Table 2. Cross-sectional openings in the Shelikof Strait region of the Gulf of Alaska.

Peninsula Location	Kodiak Location	Length (km)	Area (km^2)	Average Depth (m)
Cape Douglas	near Wonder Bay	45.971	6.504	141.5
Cape Ugyak	Cape Raspberry	46.723	8.931	191.2
Cape Kuliak	Cape Ugat	36.434	7.275	199.7
Cape Atushagvik	Cape Ugat	36.342	7.286	200.5
Cape Igvak	Cape Ikolik	75.815	14.984	197.6

There are several straits through the Kodiak archipelago between the major islands of Kodiak, Afognak and Shuyak, but these are all very narrow and shallow (Table 3). Neighboring Raspberry and Kupreanof straits, which surround Raspberry Island and divide Kodiak from Afognak Island, lead to smaller connections to the North Pacific. Raspberry Strait is interrupted by Little Raspberry Island and the passageways around it—The Slough and The Narrows—are prohibitively small (<0.001 km^2). Thus, most of the potential water exchange takes place through Kupreanof Strait, which leads to two passageways around Whale Island; Afognak Strait has a minimum cross-sectional area of 0.013 km^2 and Whale Passage has 0.023 km^2. Shuyak Strait, which divides Afognak from Shuyak Island, becomes Cape Current Narrows and has a minimum cross-sectional area of 0.008 km^2. Altogether, these Kodiak archipelago straits have a combined area of less than one percent of the minimal cross-sectional area at the northeast entrance of Shelikof, indicating that they have minimal impact on the water flow through Shelikof Strait.
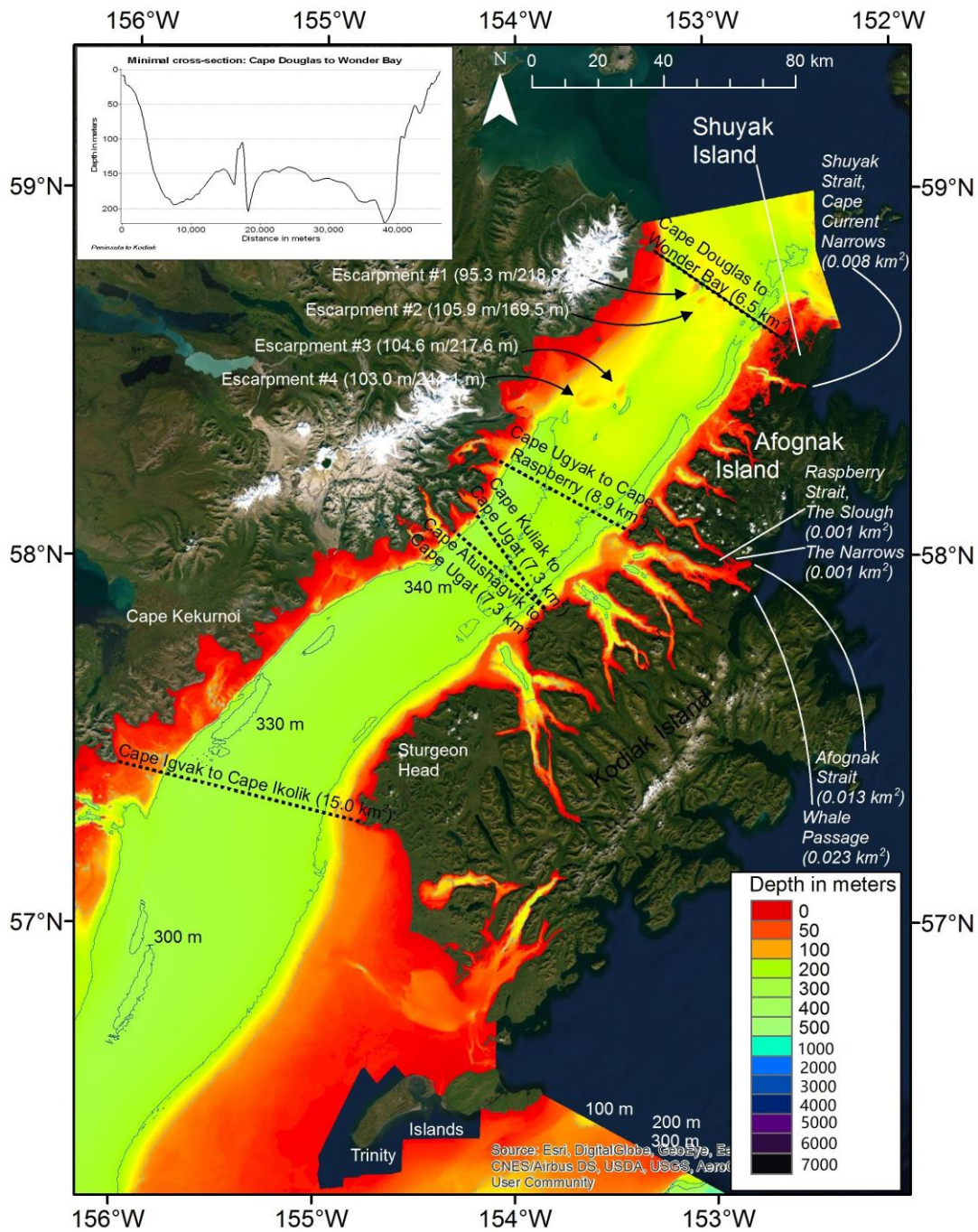
Figure 4. Cross-sections show the widest and narrowest areal openings of Shelikof Strait in the western Gulf of Alaska. Four prominent escarpments in the northwest section of Shelikof Strait are indicated along with their minimal and maximal depths. A graph shows the minimal cross-sectional opening of Shelikof Strait, ranging from Cape Douglas on the Alaska Peninsula to a location near Wonder Bay in the Kodiak archipelago.

Table 3. Cross-sectional openings within the Kodiak Archipelago of the Gulf of Alaska.

Passage Name	Length (km)	Area (km^2)	Average Depth (m)
Kupreanof Strait			
Whale Passage	1.131	0.023	19.9
Afognak Strait	1.200	0.013	10.9
Raspberry Strait			
The Slough	<0.001	<0.001	NA
The Narrows	<0.001	<0.001	0.5
Shuyak Strait			
Cape Current Narrows	0.500	0.008	15.7

3.3. Categories of Submarine Features

We mapped four broad categories of submarine features: fault scarps, shorelines, pockmarked areas, and glacial features, and we discuss identification of these features in the following section (Figure 5 is an overview map with details shown on Figures 6–13); geographic information system (GIS) data in Supplementary Information).
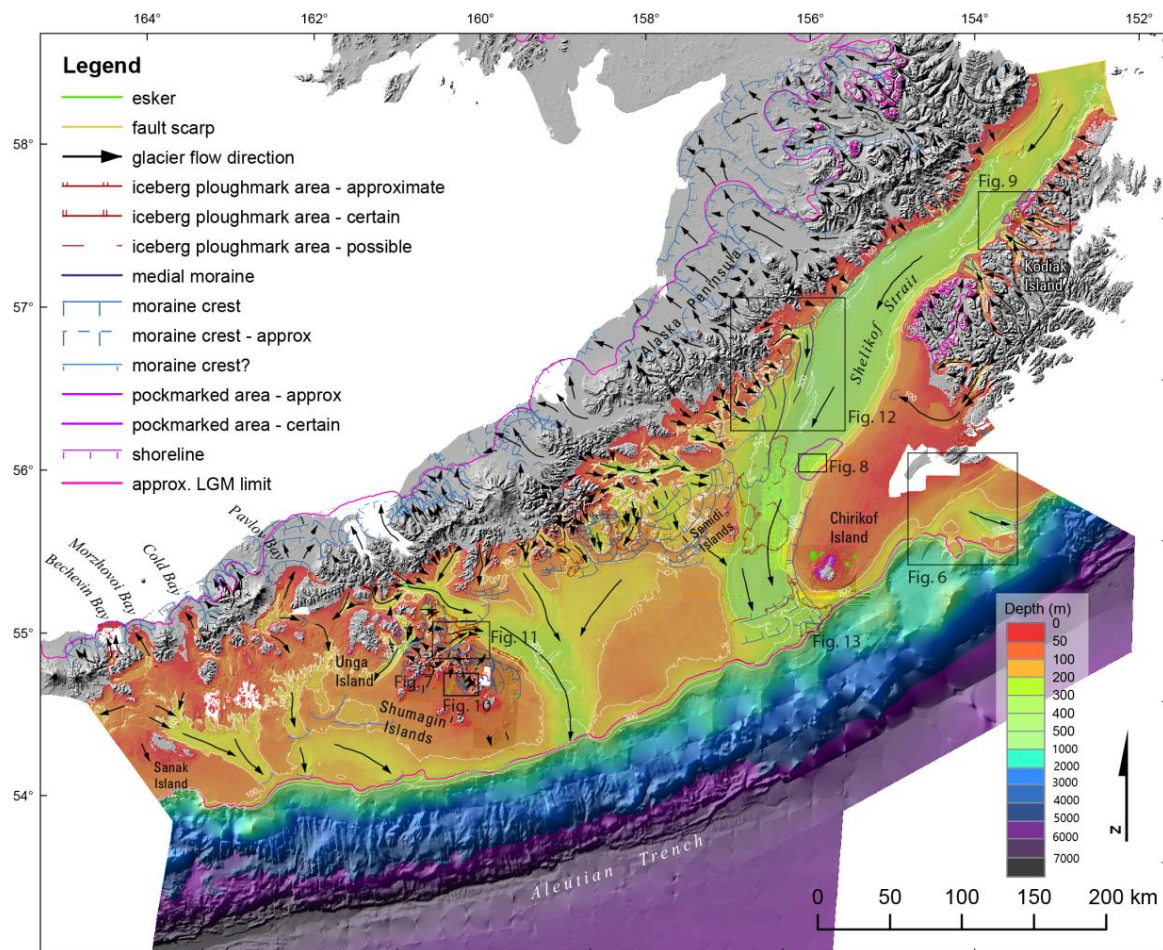
Figure 5. Geomorphic map of the Alaska Peninsula region. See text for discussion of features mapped. White lines show 100, 200, and 300 m depth contours. Last Glacial Maximum (LGM) extent shown on the north side of the Alaska Peninsula is from Kaufman et al. [46]. LGM limit on the south side of the Alaska Peninsula is from this study. Location of Figures 6–13 indicated. Geographic information system (GIS) data and larger version of map in Supplementary Information.
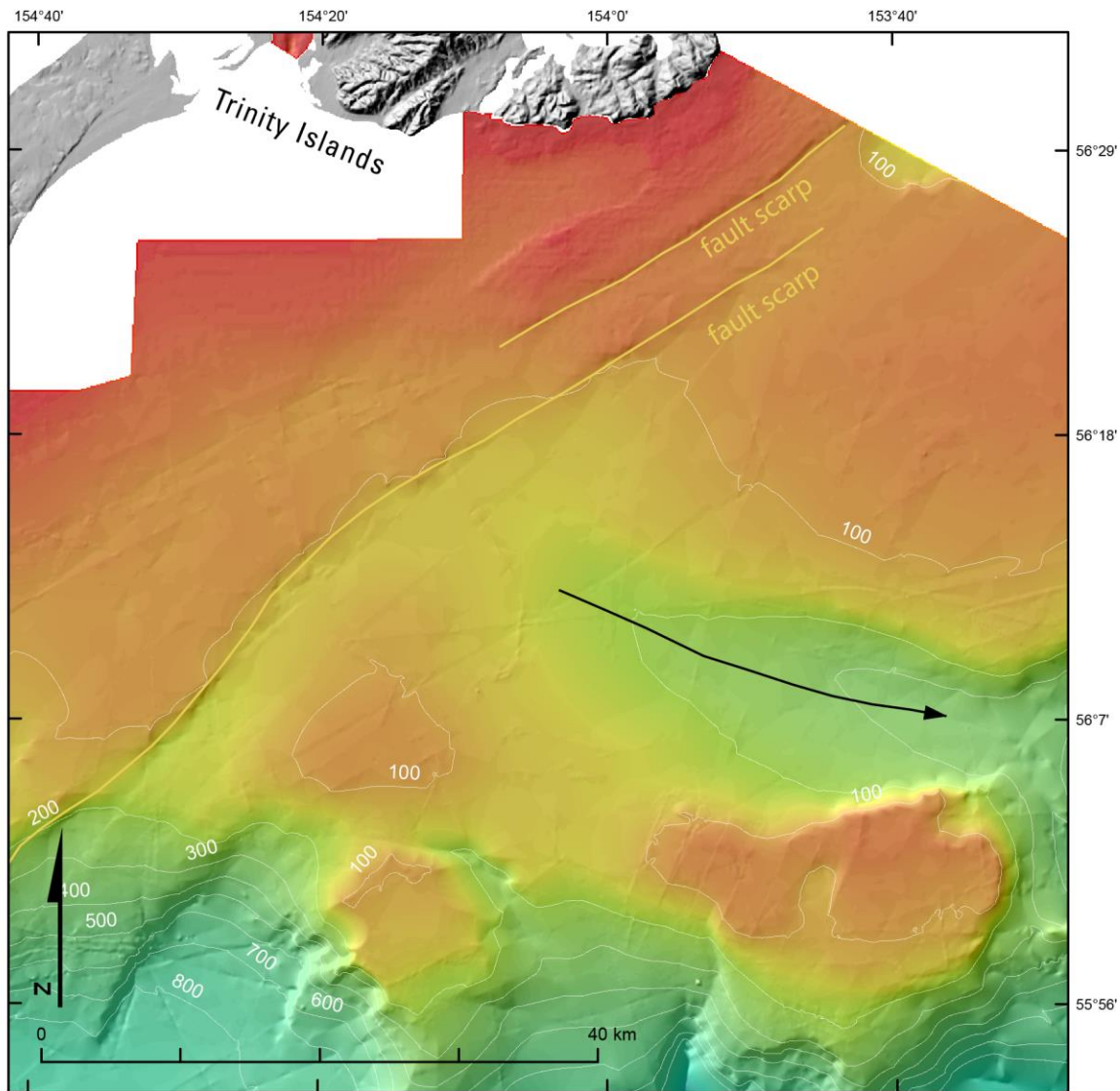
Figure 6. Yellow lines show two fault scarps in the study area to the south of the Trinity Islands, southwest of Kodiak Island. Location of the figure is shown on Figure 5 and the symbology is the same as Figure 5. The northwestern scarp is 20–25 m tall and the southeastern scarp is 40–45 m tall. See text for further discussion.

3.3.1. Fault Scarps

Only two fault scarps were identified on the sea bottom in the study area, and these are south of the southern end of Kodiak Island (Figure 6). These are long and linear features with NW-side-up scarps. The northwestern of the two scarps is 20–25 m tall and 29 km long in the region that we mapped. However, it connects with a much longer fault to the northeast that was first mapped by von Huene et al. [52]; thus the fault now appears to have a total length of 185 km. The southeastern fault scarp is less well resolved as it lies in areas of single-beam bathymetry coverage, but it appears to be 40–45 m tall and about 80 km long. Both faults are part of the Kodiak Shelf Fault Zone (KSFZ) previously identified by Carver et al. [53], initially mapped by von Huene et al. [52], and further examined by Ramos [54].
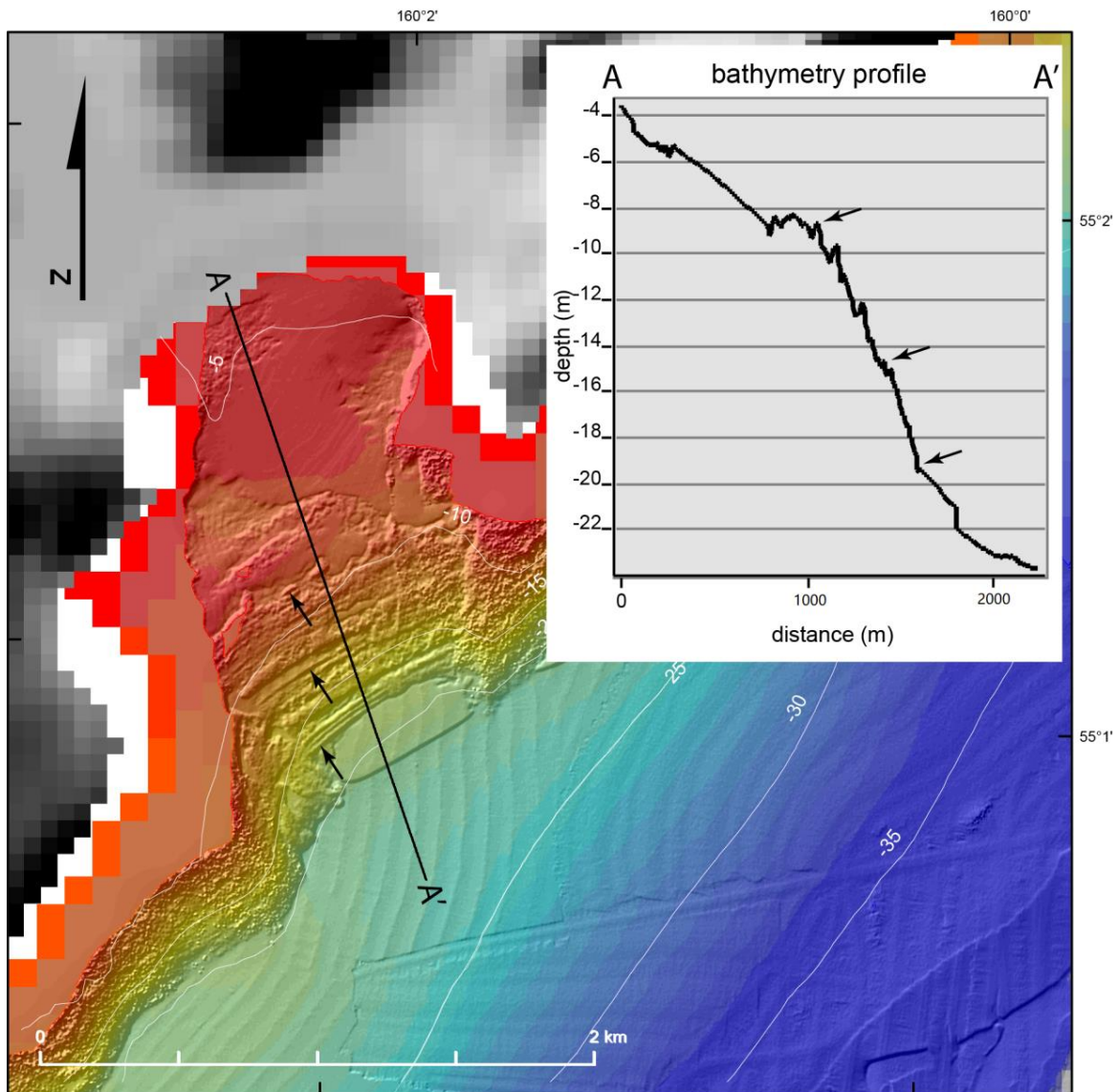
Figure 7. Submerged shorelines on southern Nagai Island. This unnamed bay lies to the southwest of Larsen Bay. The location of figure is shown on Figure 5, and the symbology is the same as Figure 5 but the color ramp is different, with the labelled contours indicating depth. Inset shows bathymetry profile with drowned shorelines between 19 m and 9 m below sea level. Elsewhere around the island, a continuous flight of shorelines extends up to 4 m below sea level.

3.3.2. Submerged Shorelines

Submerged shorelines are present in numerous locations. These are horizontal features, that are either indicative of incision into bedrock or mound-shaped, and are likely a submerged beach ridge. There is a prominent shoreline along the northwest side of Kodiak Island, on the northwest side of Chirikof Island, around southwestern Unga Island, northeastern Popov Island, and southeastern Nagai Island (Figures 5 and 7). These features were mapped at the back edge of where they incised the underlying substrate.
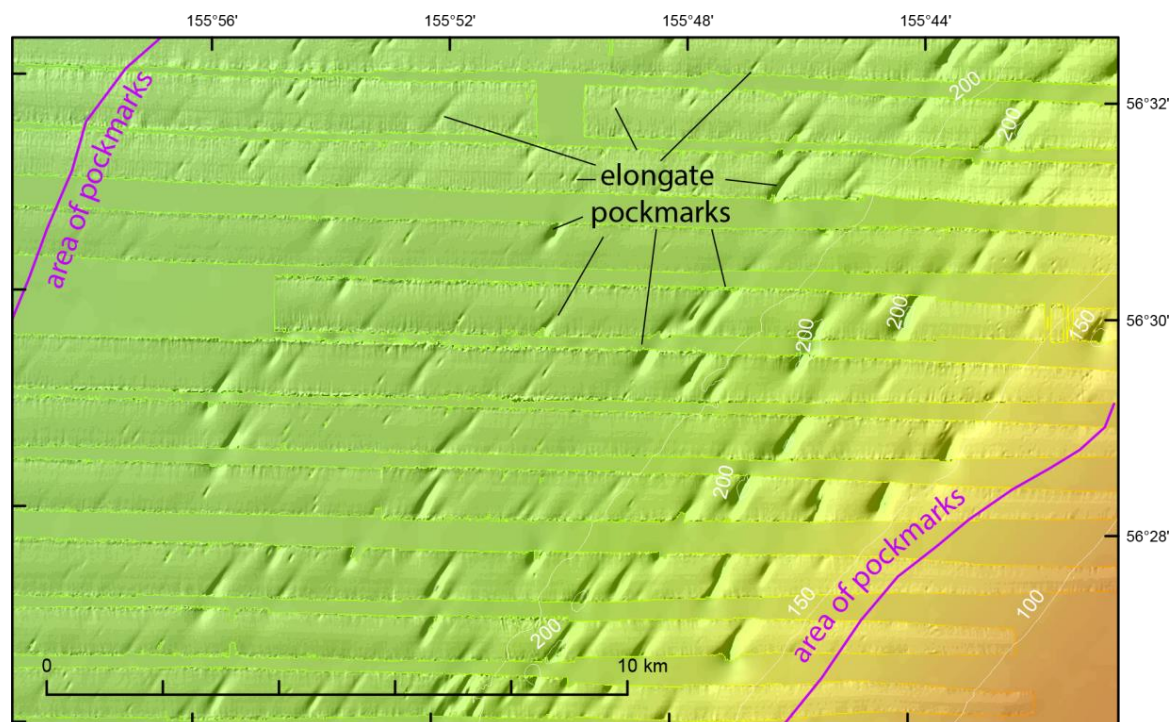
Figure 8. Pockmarked area on the east side of Shelikof Straight. Location of figure is shown on Figure 5, and the symbology is the same. These pockmarks are variable in size and are notably aligned with the glacier flow direction.

3.3.3. Pockmarks

Pockmarked areas were identified in two regions of Shelikof Strait (Figures 8 and 9). The southwestern region has pockmarks in water depths between 125 and 250 m. These pockmarks are notably elongate and parallel the glacier flow and current direction to the southwest down Shelikof Strait (Figure 8). The larger pockmarks are from 900 to 1500 m long, up to 400 m wide and up to 42 m deep. There appears to be an inverse correlation between water depth and pockmark size—the largest pockmarks are those at the shallowest water depth of the interval where they are found. The other pockmarked region west of Kupreanof Strait is different (Figure 9B). This region has circular features in 150–200 m water depths, with larger features 50–80 m across, up to 6 m deep, and they commonly have a mound on the southeast side of them that is similar in height to their depth. None of these pockmarks are in regions with iceberg ploughmarks and thus the features are unrelated.

Pockmarks are typically attributed to fluid expulsion [55,56]. Fluid expulsion can be driven by a number of factors, such as compaction of underlying sediment, gas hydrate instability, and diagenesis (see [55,56]). The origin of these pockmarks is not clear. There are no prior observations of gas hydrates in this little-studied area of Alaska. Elongate pockmarks are relatively uncommon in the literature, but ones reported suggest they tend to be larger in size [57,58]. The elongate pockmarks described by Bøe et al. [58], seem most similar to those we observe, and they infer their origin from a combination of gas seeps and bottom currents. Without sub-bottom data it is difficult to speculate further on the origin of these features.
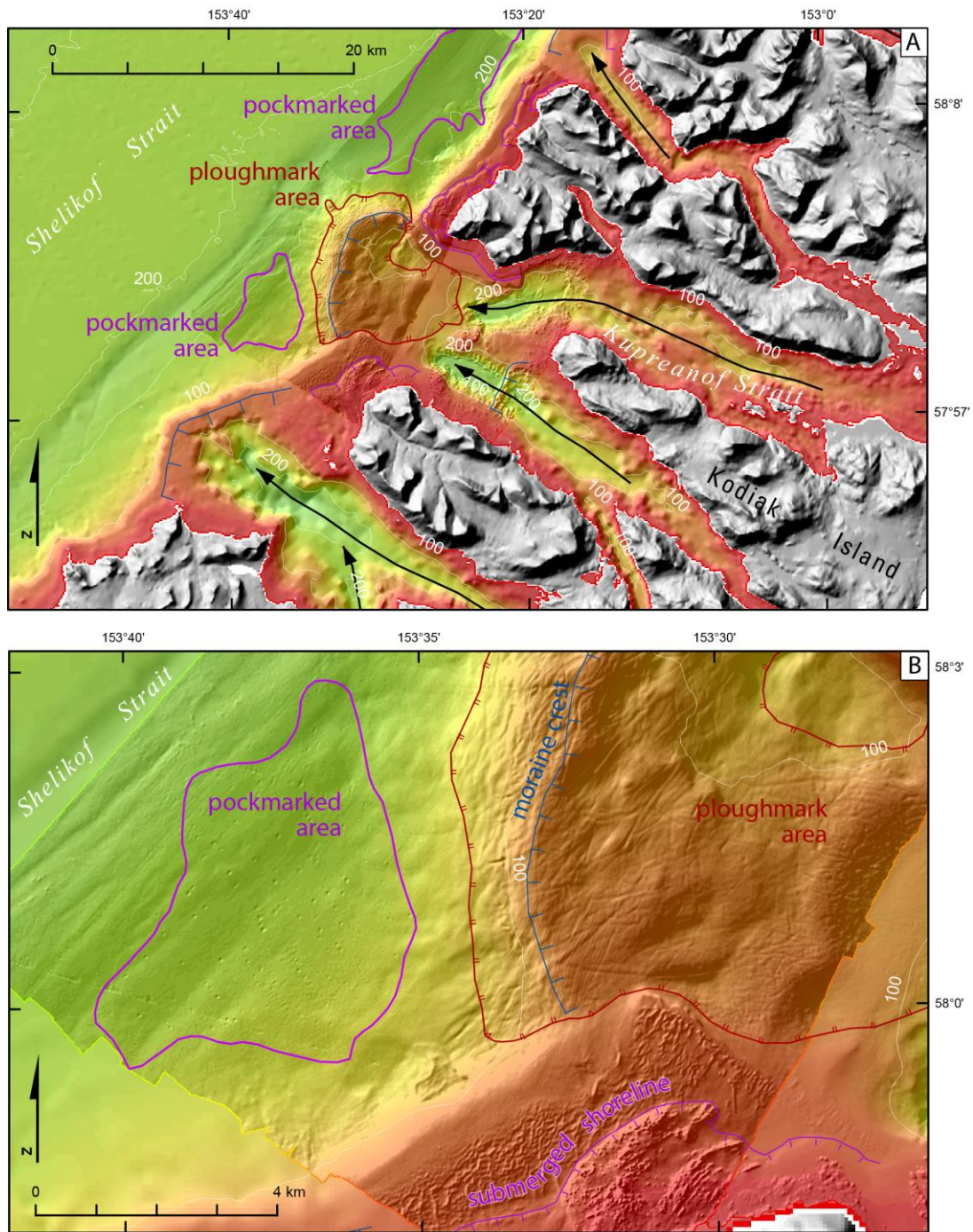
Figure 9. (**A**) Overview map of the west end of Kupreanof Strait and part of Shelikof Strait with 25 m contours. The location of the figure is shown on Figure 5 and the symbology is the same as Figure 5. This figure shows how we mapped glacier flow directions (black lines with arrowheads) down the axes of fjords. It also shows how moraine crests (blue hatchured lines) can be mapped on both high resolution and low-resolution data. Pockmarked areas (pink lines), areas with iceberg ploughmarks (red double hachured-lines), and a submerged shoreline (pink hachured line) are also shown. See text for more discussion of these features. (**B**) Expanded view of moraine at mouth of Kupreanof Strait, showing how iceberg ploughmarks extend over the crest of the moraine. Also, note the area of circular pockmarks to the west, as well as the submerged shoreline close to 50 m water depth at the bottom.
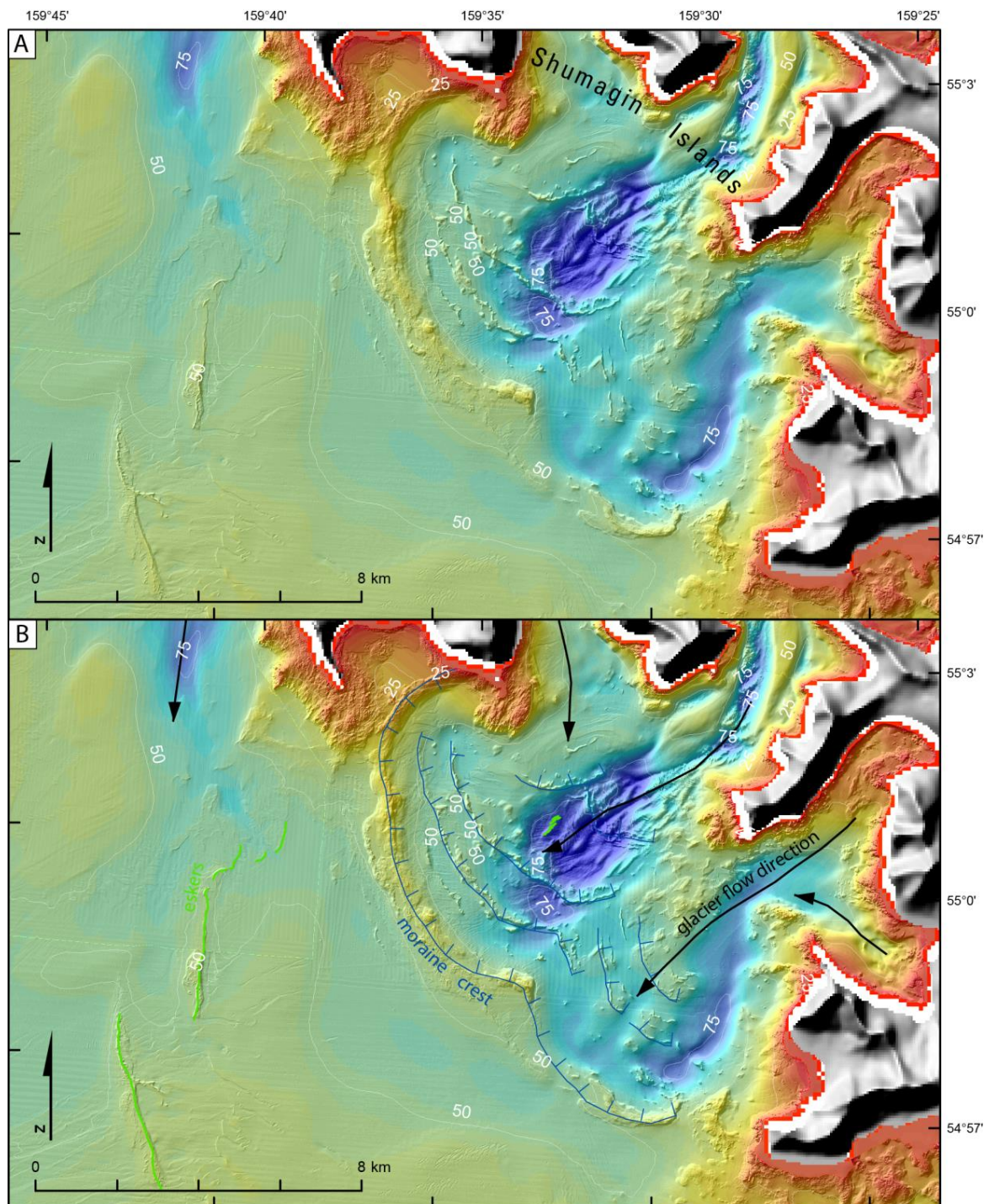
Figure 10. Glacial features mapped on the west side of the Shumagin Islands. (**A**) Bathymetry shown without interpretation, and (**B**) bathymetry shown with interpretation. Location of map is shown on Figure 5 and symbology is the same as Figure 5, but the color ramp is different, with the labelled contours indicating depth. These images show glacial lineations in the central part of the trough, the moraine crests and then some probable eskers (green lines) distal to the moraine crests.
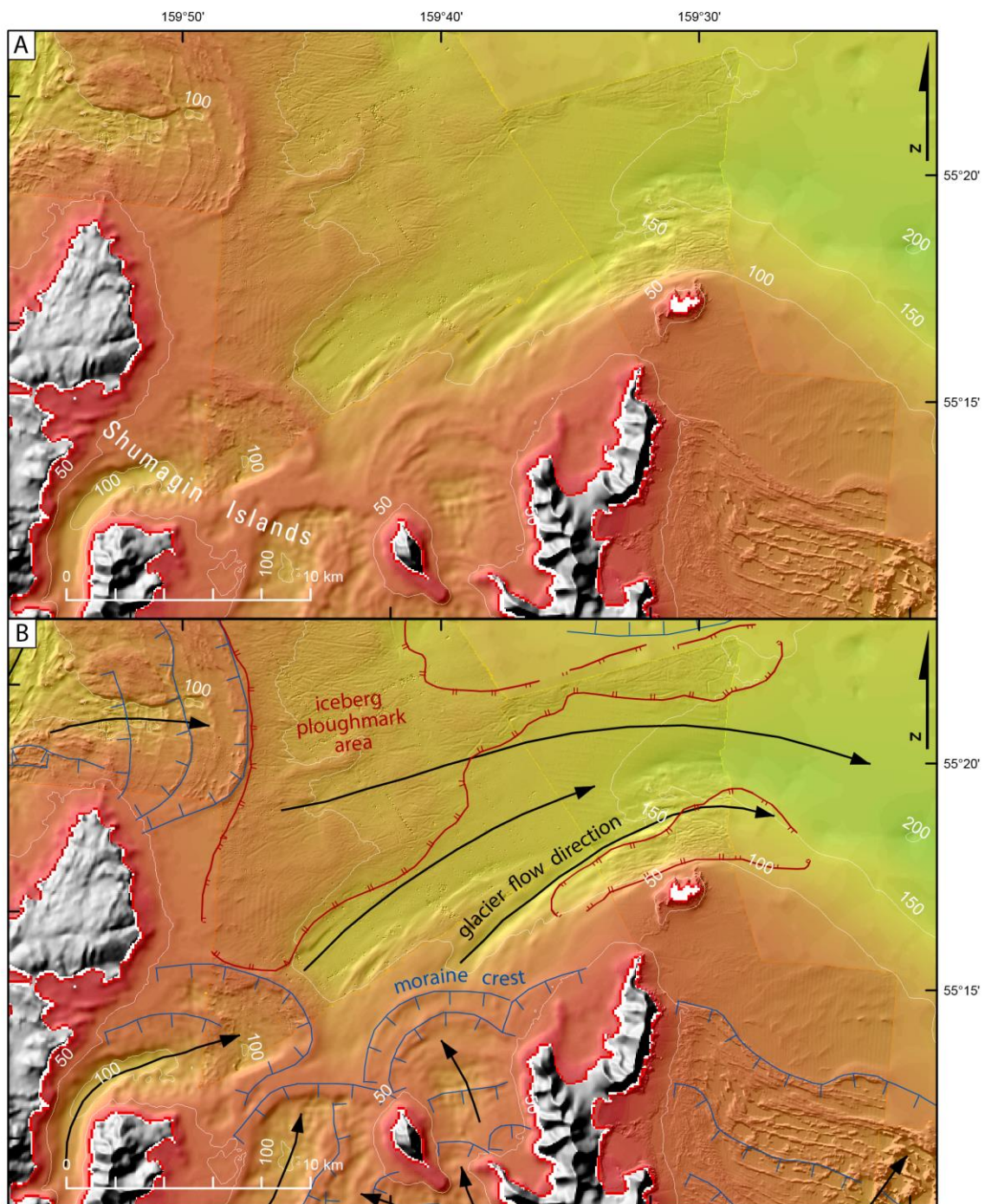
Figure 11. Glacial features on the north side of the Shumagin Islands. (**A**) uninterpreted, (**B**) interpreted. Location of map is shown on Figure 5 and the symbology is the same as Figure 5. This region is notable for having abundant parallel recessional moraines, in the bottom right part of the map, and the glacial lineations distal to the prominent moraines. At the top, there are iceberg ploughmarks adjacent to the prominent moraine crest, and the dominant ploughmark direction is away from the moraine crest, all of which suggests that the glacier was a tidewater glacier.
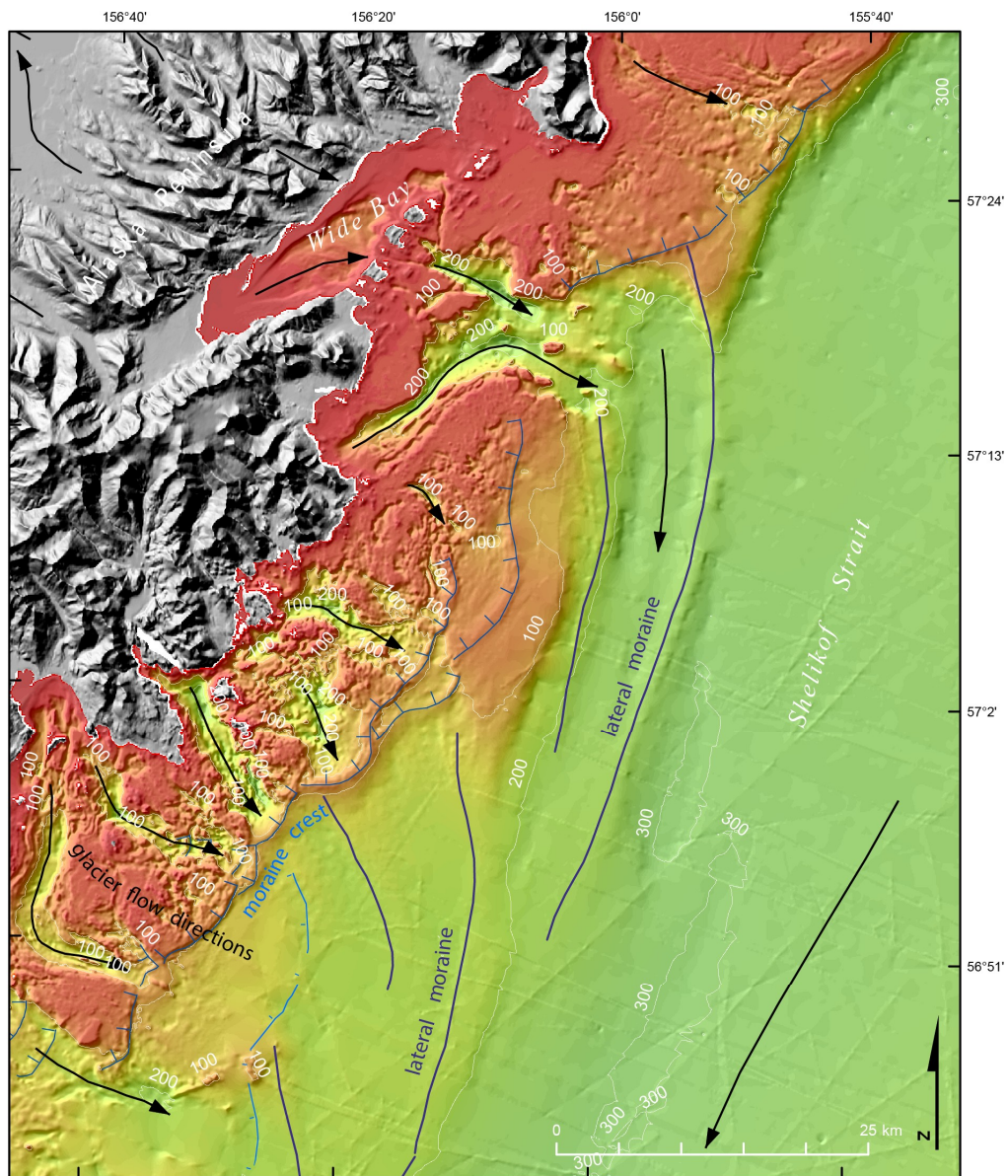
Figure 12. Moraine crests, medial moraines, and ice flow directions along the west side of Shelikof Strait. Location of map is shown on Figure 5 and the symbology is the same as Figure 5. This region is notable for the well-defined medial moraines. Other moraine crests are more subtle on the bedrock regions of the shelf where the sea bottom has a planar and chaotic morphology.
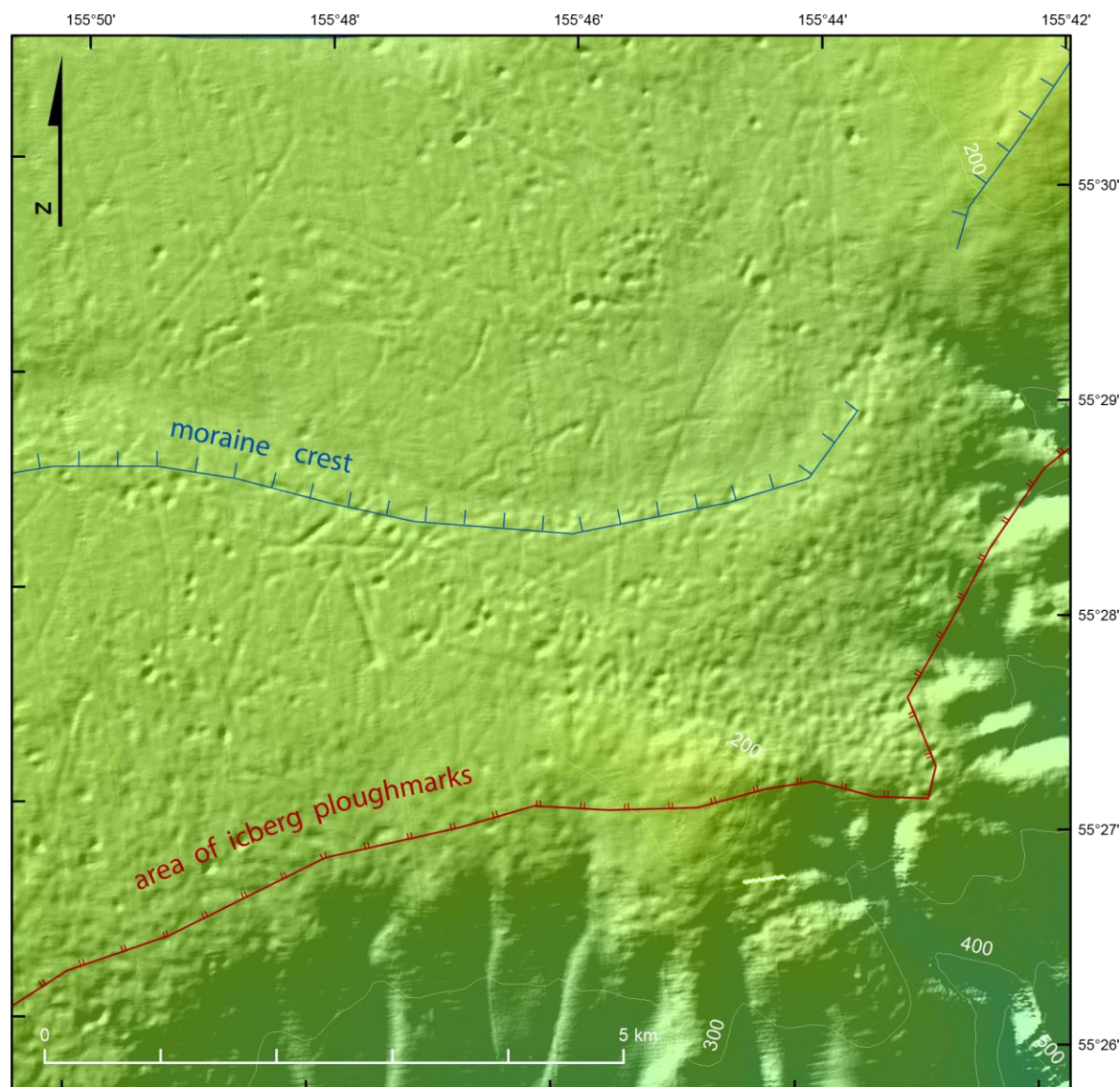
Figure 13. Iceberg ploughmarks on the moraine at the mouth of Shelikof Trough. Location of map shown on Figure 5 and symbology is the same as Figure 5. Some of the grooves in this area are up to 5.5 km long and 7 m deep in 200–250 m water depth.

3.3.4. Glacial Features

For glacial features, we mapped five types of features: moraine crests, medial moraines, glacier flow directions, eskers, and iceberg ploughmarks (Figures 5 and 9–13). For typical terrestrial mapping of moraines, the distal position of moraines are mapped, because the entire moraine complex and outwash fans can often be observed. For submarine moraines imaged with the multibeam bathymetry (e.g., similar to moraines in studies in Dowdeswell et al. [59] (2016), and Otteson and Dowdeswell [60], 2006), we could map similar distal positions of moraines, but the resolution of the single-beam bathymetry is not sufficient to map the distal position of moraines. However, moraine crests can be confidently identified, and thus we mapped moraine crests, not the distal extent of the moraines, throughout the datasets. We did not attempt to map every moraine crest. In particular in the Semidi-Shumagin Island region where there are numerous recessional moraines (Figures 5, 10 and 11), and given the reconnaissance nature of the mapping for this study, we only mapped enough moraine crests to give the reader a sense of their geometries. We encourage further examination of the original NOS multibeam datasets. Also mapped were a few medial moraines. The largest are up to 30 m tall along the west side

of Shelikof Strait (Figure 12), which are clearly imaged even with the low-resolution data. Glacier flow directions could also be identified in several ways. In some areas, glacier flow sculpted drumlinoid features and elongate glacial lineations.

In other instances, elongate lineations indicate the glacier flow direction (Figures 10 and 11), similar to features observed near Svalbard (Ottesen and Dowdeswell [60], 2006; Dowdeswell et al. [59], 2016). Lastly, the orientation of elongate basins and troughs identified glacier flow directions (Figures 5, 6 and 9–12). Eskers, a fluvial deposit of gravel beneath a stagnating ice sheet, were identified in a number of locations, are commonly 2–4 m tall, but range up to 14 m tall and up to 2.6 km long (Figure 10). These were identified by their distinctive positive topography and meandering form, and are consistent in morphology to eskers observed in other submarine environments (Ottesen et al. [61], 2008; Dowdeswell et al. [59], 2016). Kaufman et al. [46] and Kaufman and Manley [38] mapped the LGM glacial extent at roughly the shelf-slope break. With our improved bathymetry compilation, their mapped southern position of ice wandered across the shelf-slope break. We remapped the position of the LGM extent in the study area to the shelf-slope break based on our better dataset (Figure 5).

Lastly, iceberg ploughmarks—grooves formed by scraping of icebergs along the ocean bottom [62,63]—are present in 13 different areas within the study area (Figures 5, 9, 11 and 13). These grooves are commonly less than 1–1.5 m in depth, but a few are 4–7 m deep. One mark was 5.5 km long, and other noticeably long ploughmarks were 3–3.5 km long. The prominent ploughmarks are commonly 70–95 m wide and 115 m was the maximum measured width. Ploughmarks are found on both sides, and on the crest, of the moraine near the west end of Kupreanof Strait (Figure 9), indicating a tidewater glacier during moraine formation and deglaciation. Just north of the Shumagin Islands (Figure 11), the iceberg ploughmarks extend up to the moraine crest, also indicating that there was a tidewater glacier there. At the mouth of Shelikof Strait, both ploughmarks and iceberg pits are found, indicating stagnating ice (Figure 13). Iceberg pits form when melting icebergs turn over and impact the sea bottom, forming circular or semi-circular depressions (e.g., [64]). These pits often have lips adjacent to the depression related to the movement of sediment by the turning or impacting keel, which is what we find for these pits. We note that our observations are limited to areas less than ~250 m water depth as we had no high-resolution multibeam data from the slopes beyond the shelf break. We compared our areas of mapped and inferred ploughmarks to our 100 m bathymetric model of the study area, and then computed a histogram, divided into 1 m depth bins, for the ploughmark depths (Figure 14). The peak of ploughmark abundance is at 211 m water depth. Without knowing more about the amount and timing of GIA (glacial isostatic adjustment) and relative sea level rise, it is difficult to infer the size of the icebergs. However, if we were to assume that the amount of crustal depression is 65–135 m [40], and that at LGM time, sea level was 121 m below the present day level [65], then most icebergs would have been grounding in 155 to 197 m water depth, indicating there were many large icebergs. This is the first identification of iceberg ploughmarks along the southern Alaska margin. With acquisition of additional multibeam datasets, it seems likely that more ploughmark fields will be identified.
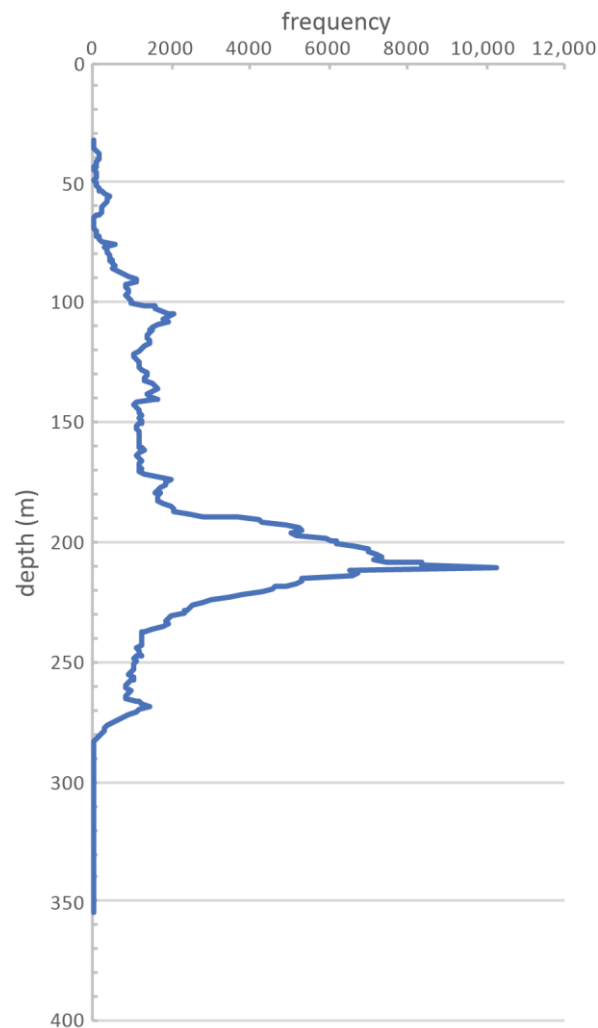
Figure 14. Histogram of ploughmark digital elevation model (DEM) depths in study area. Regions of ploughmarks where mapped in the study area were binned in 1 m depth intervals using the overall 100 m western Gulf of Alaska bathymetry dataset, and then the histogram constructed of those depths.

4. Discussion

High-quality seafloor mapping data, such as that acquired by multibeam and sidescan sonar systems, are generally required for geological description of significant seafloor features. Our combination of various multibeam, LIDAR, pre-multibeam hydrographic smooth sheets, and numerous uncalibrated underway files from fishery research vessels and chartered fishing vessels proved adequate for tracing the course of ancient ice masses. While this is the sixth, large, regional, seafloor compilation of Alaska that we have published, it is the first to undergo significant geological analysis. Interpretation of glacial features began with the higher-quality, shallow-water multibeam data and then was extended outward to include lower quality data sets, such as the smooth sheets and single-beam, indicating successful integration of several independent bathymetry data sources. Our choice of producing a 100 m horizontal resolution depth grid is supported by 32.9% of grid cells being based on actual depth observations, a value that is nearly double that of GEBCO's global 18% being based on actual depth observations [14]. This difference is because much of our very small study area was in shallower waters that are much more suitable to measuring depths and because we had access to our own institution's numerous fishery research cruise underway files.

4.1. Improved Bathymetry for Oceanography and Fisheries Research

Numerous fishery-oceanography studies have investigated the flow of waters in Shelikof Strait and the impact of those flows on the annual winter spawning of walleye pollock due to its economic and ecological importance. Collectively, the Alaska stocks of walleye pollock from the Gulf of Alaska, Aleutian Islands and eastern Bering Sea support the largest fishery in the world [66], contributing to the global food supply. The Alaska Coastal Current (ACC) is the dominant water transport feature in the strait, and it has a mean surface transport of 0.85×10^6 m^3 s^{-1} to the west [67], while deep waters from the Gulf of Alaska flow into the strait in the opposite direction [68]. Strong wind events can temporarily triple this ACC flow and eddies frequently form within the strait [69], sometimes entraining larval pollock and providing them with good survival [70]. An analysis of 28 years of Shelikof Strait ichthyoplankton cruises has shown that egg density increases at the periphery of the spawning area in years with higher spawner biomass, transport of the eggs to the west increases with increased ACC flow, and egg density is positively correlated with depth [71]. Oceanographic calculations such as water flows depend on appropriate placement of moorings and knowledge of minimum cross-sections and maximum depths. All Shelikof Strait oceanographic calculations appear to rely on a single estimate of the location ("upper strait" p. 6680, [72]), maximal depth (175 m), and cross-sectional size (6×10^6 m^2) of the narrowest pass within Shelikof, although there does not appear to be any formal analysis for determining this information [72]. Our new bathymetry clearly defined the location of the smallest cross-section, determined that its maximal depth (221.1 m) is deeper than previously estimated, and showed that it is 7.7% larger (6.5×10^6 m^2) than previously estimated. Hopefully, our new WGOA bathymetry can be used for future WGOA oceanographic work for improving our understanding of walleye pollock spawning success in Shelikof Strait.

The population of the Pacific sleeper shark, a rare but large-growing species (reaching 7.6 m in length; [73]), has a great affinity for Shelikof Strait. Unfortunately, little is known about the influences on its abundance and distribution; it is not formally assessed as a species for fishery management purposes (grouped into the generic shark category in the GOA: [74]), nor is its EFH assessed [23]. Over the history of the GOA bottom trawl survey (1984–2017, data available at https://www.afsc.noaa.gov/RACE/groundfish/survey_data/default.htm), nearly half (44%) of all GOA research hauls with sleeper sharks and 56% of all GOA sleeper shark biomass have come from Shelikof Strait. Another, much smaller concentration (9%) occurs south of False Pass in much shallower water (mean depth = 93 m). While the catch has never been widespread across the GOA, in the five most recent GOA biennial trawl surveys (2009–2017), all sleeper sharks caught were in the Shelikof Strait and False Pass areas, with the exception of a single catch in 2011 that occurred between the two areas. An analysis of bycatch from the sablefish longline survey covering the eastern Bering Sea slope, the Aleutian Islands, and the Gulf of Alaska showed 54% of all sleeper shark catch occurred in Shelikof, increasing over the course of the entire analysis (1979–2003) [21]. Thus, there is some unknown link between the Pacific sleeper shark and Shelikof Strait, and our new WGOA bathymetry should help improve our understanding of its main Alaska habitat.

4.2. Improved Bathymetry for Updating Larger Compilations

Our new bathymetry of Shelikof Strait and the surrounding WGOA may also provide a helpful update for larger bathymetry compilations such as GEBCO (General Bathymetric Chart of the Oceans: [14]), which is being updated in an effort entitled the "Nippon Foundation GEBCO Seabed 2030 Project" [75]. GEBCO, along with the ETOPO2 (Earth Topographic) [76] and ETOPO1 compilations [16], has relied on partially calibrated satellite altimetry data for much of its coverage and lacked local bathymetry sources, such as the underway cruise files that we utilized, and therefore sometimes has insufficient groundtruthing. To illustrate the potential utility of our new WGOA bathymetry compilation, we provide bathymetry maps of the same area from six previously published sources and also provide depth difference maps. Depth difference maps were created simply by subtracting an external bathymetry compilation from our compilation such that results are available

in positive or negative meters. Positive differences indicate that the other source was deeper than our compilation while negative differences indicate that the other source was shallower than our compilation. Bathymetry and depth difference maps are included for GEBCO [14] (Supplements 2 and 3, respectively), ARDEM (Alaska Regional Digital Elevation Model) [17] (Supplements 4 and 5, respectively), ETOPO2 [76] (Supplements 6 and 7, respectively), ETOPO1 [16] (Supplements 8 and 9, respectively), AKRO 2005 (Supplements 10 and 11, respectively), and AKRO 2017 (Supplements 12 and 13, respectively).

4.2.1. Machine versus Human Processing

Most bathymetry compilations process huge quantities of data and rely on computer algorithms and automated outlier detection to remove errors. Global bathymetry compilations also rely on calibrating satellite altimetry data with real depth observations, and lack of local depth soundings of an area hampers this correction process. We do not rely on automated outlier detection nor satellite gravity measurements for our bathymetry compilations. Instead, we process our data sets individually, comparing them against source documents, if possible, to find and fix or remove outliers. Thus our WGOA bathymetry compilation benefited greatly from the careful smooth sheet data editing that we routinely perform [50], the multibeam processing of previously incomplete surveys, and from the editing and incorporation of numerous ship track or underway files not readily available for other compilations.

For example, the GEBCO compilation shows a ~4200 m deep hole in an area just west of the Semidi Islands (Supplement 2) where we have depths of ~140 m (Figure 3) from NOS multibeam survey H11465, and GEBCO also has ~200–400 m deep depressions near the Shumagin Islands and Chirikof Island (Supplement 2) where we have very shallow water (Figure 3). GEBCO was generally shallower in Shelikof Strait and the south side of the Aleutian Trench and deeper on much of the shelf and north side of the Aleutian Trench (Supplement 3). The ARDEM compilation [17] (Supplement 4), derived mostly from NOS hydrographic charts, is coarser but generally in agreement with our WGOA compilation, except in areas of sparse chart soundings. As in GEBCO, the ARDEM was shallower on the south side of the Aleutian Trench and deeper on the north side of the Aleutian Trench (Supplement 5). The ETOPO2 bathymetry (Supplement 6) was 10 to 100 m deeper and shallower across large, homogenous areas of the shelf and Shelikof Strait (Supplement 7), perhaps indicating regional differences in gravity. The ETOPO1 bathymetry (Supplement 8) was more variable, with smaller areas of homogenous 10 to 100 m depth differences (Supplement 9) than ETOPO2. Similar to the GEBCO and ARDEM bathymetry, ETOPO1 was shallower on the south side of the Aleutian Trench and deeper on the north side. The coarse AKRO 2005 bathymetry (Supplement 10) had large areas on the inner shelf of general agreement with our bathymetry that roughly corresponded to areas of smooth sheet coverage (Figure 2), but also large areas of 10 to 100 m depth differences on outer shelf areas without smooth sheet data (Supplement 11). The detailed AKRO 2017 bathymetry (Supplement 12) had several straight lines, presumably vessel track lines that were deeper or shallower than the surrounding bathymetry (Supplement 13), most notably in Shelikof Strait and on the outer shelf, mostly outside of the smooth sheet coverage. Similar to the AKRO 2005, the AKRO 2017 also had large areas of 10 to 100 m depth differences on the outer shelf, such as a rectangular patch around the northern Semidi Islands that was 10 to 100 m too deep (Supplement 13).

4.2.2. Unnamed Bank

Another area of cartographic confusion has been the unnamed and unsurveyed bank that is located between the trough mouths of Shelikof Trough and Shumagin Trough (Figure 3). By extracting and editing numerous underway files, we show this bank is relatively flat, shallower than 100 m, and rising to about 75 m at its shallowest. The flatness of the bank indicates that it was not sculpted by the main cross-shelf glaciers. The GEBCO compilation [14] (Supplement 2) has a hole about 10 km across and reaching a maximum depth of 173 m in the northwest area of the bank along with a shallow

ridge that reaches a minimum depth of 29 m near the northwestern edge of the bank. ARDEM [17] (Supplement 4) has a peak of 67 m at a location we have as about 95 m, a few low spots deeper than 100 m, and an area off the south side of the bank close to 100 m where we have depths of about 190 m. ETOPO2 [76] (Supplement 6) shows the entire bank as being deeper than 100 m and exceeding 200 m in depth on its northeast side. ETOPO1 [16] (Supplement 8), shows a more uneven bank, with four large depressions ranging down to about 180 m deep and three large shallow areas ranging up to 1 m in depth. The NMFS AKRO bathymetry compilation (variable resolution, 2005), has three large banks within this same bank rising to a depth of 4 m (Supplement 10), while an updated version (40 m resolution, 2017) reduces the extent of these shallow spots, but also adds some depressions approaching 180 m in depth (Supplement 12). The AKRO 2017 also has several ship tracks crossing the bank, roughly matching the depths of our soundings in this area, but often about 50 m deeper or shallower than the other soundings used by AKRO 2017 to define this bank, creating linear walls or trenches.

4.2.3. Shelikof Escarpments

The four small escarpments that we describe in the northeast end of Shelikof Strait (Figure 4) are also difficult to identify in many of these larger compilations. Our bathymetry compilation indicates that there are four distinct blocks, which have a rounded form, suggesting that they may be heavily draped in sediment. Future investigations may determine their origin as bedrock knobs, glacial deposits, or blocks from volcanoes to the northwest. ETOPO2 [76], at an east–west resolution of about 1900 m and a north-south resolution of about 3700 m, does not show any evidence of them at all (Supplement 6). ETOPO1 [16], with improved east-west (~950 m) and north–south resolutions (~1900 m), shows the peaks of the escarpments quite clearly, but is still too coarse to depict the deeper areas of the nearby bays on the north side of Afognak Island (Supplement 8). GEBCO [14] also depicts the four escarpments, and adds some detail to the Afognak bays, but adds two smaller peaks on the flat Shelikof Strait seafloor approaching the Barren Islands (Supplement 2). The AKRO bathymetry compilation (variable resolution, 2005) shows the northern two escarpments, smooths away the southern two escarpments, and adds an additional rising to a depth of 5.5 m on the seafloor near Shuyak Strait where we have depths of about 200 m (Supplement 10). An updated (2017) AKRO compilation (https://alaskafisheries.noaa.gov/) depicts all four escarpments quite clearly but has a 155 m deep hole in the northernmost one, and keeps the two seafloor peaks from GEBCO and the third one from the previous AKRO compilation (Supplement 12). There are also two distinct ship tracks, about 10 m deeper than the other soundings, running parallel down the center of the strait in the AKRO 2017 compilation (Supplement 12), which show up as trenches in the depth difference map (Supplement 3). ARDEM [17] shows the four escarpments clearly despite its ~1000 m resolution (Supplement 4) and does not show any other seafloor peaks in the area.

4.3. Glacial Geomorphology

Our combined map of onshore and offshore glacial features provides the first synoptic view of glaciation of the Alaska Peninsula region. There is clearly a rich record of glaciation on the shelf south of the Alaska Peninsula, with the preservation of numerous moraine crests, eskers, shorelines, and iceberg ploughmarks. The presence of the iceberg ploughmarks indicates deposition of virtually no sediment onto these areas since their formation sometime prior to roughly 10,000 years ago, which is consistent with findings elsewhere along the southern Alaska margin [77].

The glacier flow directions provide evidence for the location of the maximum thickness of ice along the Alaska Peninsula. In particular, the northward looping moraines at Bechevin Bay, Morzhovoi Bay, Cold Bay, and Pavlov Bay have long been recognized as indicating there was an ice cap offshore to the south of the Alaska Peninsula (Figure 1) [38,40,42–45]. We infer the crest of this ice cap was approximately in the region southwest of Deer Island, and we refer to this as the "Cold Bay ice cap". Further offshore, the ice flow directions are to the southwest and southeast, indicating that the ice

cap must have lain to the northwest. Further to the northeast, the topographic crest of the Alaska Peninsula is simply the divide between northwest-flowing and southeast-flowing ice masses.

Some glaciations were far more extensive than others. Clearly the glaciation that filled the Shelikof Trough was the most extensive of any in the region (Figure 5), and these cross-shelf troughs are inferred to be the location of ice streams when ice was to the edge of the continental shelf [78]. Moreover, much of the ice that flowed down Shelikof Strait was sourced from the Cook Inlet and Alaska Range regions [79]. Several large medial moraines are present along the west side of Shelikof Strait. Presumably, a large glacier exited Wide Bay and flowed to the south, generating a medial moraine between the main trunk of the Shelikof Strait glacier and the Wide Bay glacier. Several other medial moraines are in the offshore region due south of Wide Bay, beneath the west side of Shelikof Strait. Another large depression, which we refer to as the Shumagin Trough, lies just east of the Shumagin Islands. This large glacial trough extends about 175 km from the crest of the Alaska Peninsula to the shelf edge. Ice likely extended westward from the Semidi Islands and joined the main ice in the Shumagin Trough. There is another significant glacial trough just east of Sanak Island, which we refer to as the Sanak Trough. This depression also emanated from the Cold Bay ice cap. Less-extensive glacial limits are also evident. Moraines surround the outer Shumagin Islands and numerous recessional moraines are preserved—particularly on the northeast side of the islands. Similarly, larger moraine crests and numerous recessional moraines also lie west of the Semidi Islands.

The different extents of moraines leads us to consider their ages. As previously stated, our focus of this paper is descriptive, and not interpretive. The terrestrial moraines mapped on the north side of the Alaska Peninsula [42–45] can be divided into two categories—those older than the limit of radiocarbon dating (roughly 40,000 years) and those younger. The younger moraines terminate mostly on land, whereas the older ones at least partially terminate offshore on the peninsula. There seems to be no simple pattern to relate these dated moraines to the submarine features. The simplest interpretation is that most of the submarine glacial features are related to LGM glaciation, where glaciers were at their maximum positions from around 26,000 to 20,000 or 19,000 years ago [47]. If Kaufman et al.'s [46] assumption is correct that LGM glaciers went to the shelf-slope break, then morphologic evidence of older glaciations was likely completely erased from the region. Another possibility is that LGM glaciers did not make it that far seaward, and that the largest glaciers were limited to the cross-shelf troughs. Work on Sanak Island (Figure 1) indicates retreat of ice from the island just prior to 17,000 years ago [39], suggesting rapid retreat of ice from the Sanak trough between ~20,000 and 17,000 years ago. The distinct and well-defined moraines surrounding the Semidi and Shumagin Islands may reflect re-expansion of ice sheets at the beginning of Younger Dryas time as documented elsewhere in southern Alaska [41,80,81]. Additional multibeam bathymetry, high-resolution seismic data, and cores would help to clarify all these questions related to the ages of moraines, deglaciation, GIA and sea level rise. Lastly, given the abundance of sea-floor features from LGM time, such as the iceberg ploughmarks, we infer Holocene sedimentation rates on parts of this margin are low, and thus it seems future coring efforts would be fruitful in clarifying the glacial history of the region.

References

1. Frost, O.W. *Bering: The Russian Discovery of America*, 1st ed.; Yale University Press: New Haven, CT, USA, 2003.

2. Golder, F.A. *Bering's Voyages*, 2nd ed.; Conde Nast Press: New York, NY, USA, 1935.

3. Postnikov, A.V.; Falk, M.W. *Exploring and Mapping Alaska: The Russian American Era, 1741–1867*, 1st ed.; Black, L., Translator; University of Alaska Press: Fairbanks, AK, USA, 2015.

4. Beaglehole, J.C. *The Life of Captain James Cook*, 1st ed.; Stanford University Press: Stanford, CA, USA, 1974.

5. McCormick, J. *Geographic Dictionary of Alaska*, 2nd ed.; US Geological Survey Bulletin: Washington, DC, USA, 1906; Volume 299, p. 690.

6. Orth, D.J. *Dictionary of Alaska Place Names*; Professional Paper 567; US Geological Survey: Washington, DC, USA, 1967; p. 1084.

7. Jones, E.L. *Safeguard the Gateways of Alaska: Her Waterways*; U.S. Department of Commerce, U.S. Coast and Geodetic Survey, Special Publication No. 50; U.S. Government Printing Office: Washington, DC, USA, 1918.

8. Belknap, G.E. *Deep-Sea Soundings in the North Pacific Ocean Obtained in the United States Steamer Tuscarora*; United States Hydrographic Office No. 54; U.S. Government Printing Office: Washington, DC, USA, 1874.

9. Tanner, Z.L. *Explorations of the Fishing Grounds of Alaska, Washington Territory, and Oregon, During 1888, by the U.S. Fish Commission Steamer Albatross*; Bulletin of the United States Fish Commission Volume 8, for 1888; U.S. Government Printing Office: Washington, DC, USA, 1890.

10. Zimmermann, M.; Prescott, M.M.; Rooper, C.N. *Smooth Sheet Bathymetry of the Aleutian Islands*; U.S. Department Commerce: Washington, DC, USA, 2013.

11. Zimmermann, M.; Prescott, M.M. *Smooth Sheet Bathymetry of Cook Inlet, Alaska*; U.S. Department Commerce: Washington, DC, USA, 2014.

12. Zimmermann, M.; Prescott, M.M. *Smooth Sheet Bathymetry of the Central Gulf of Alaska*; U.S. Department Commerce: Washington, DC, USA, 2015.

13. Zimmermann, M.; Prescott, M.M. Bathymetry and Canyons of the Eastern Bering Sea. *Geosciences* **2018**, *8*, 184. [CrossRef]

14. Weatherall, P.; Marks, K.M.; Jakobsson, M.; Schmitt, T.; Tani, S.; Arndt, J.E.; Rovere, M.; Chayes, D.; Ferrini, V.; Wigley, R. A new digital bathymetric model of the world's oceans. *Earth Space Sci.* **2015**, *2*, 331–345. [CrossRef]

15. Smith, W.H.F.; Sandwell, D.T. Global seafloor topography from satellite altimetry and ship depth soundings. *Science* **1997**, *277*, 1957–1962. [CrossRef]

16. Amante, C.; Eakins, B.W. ETOPO1 1 Arc-Minute Global Relief Model: Procedures, Data Sources and Analysis. In *NOAA Technical Memorandum ESDIS NGDC-24*; NOAA: Silver Spring, MD, USA, 2009.

17. Danielson, S.L.; Dobbins, E.L.; Jakobsson, M.; Johnson, M.A.; Weingartner, T.J.; Williams, W.J.; Zarayskaya, Y. Sounding the northern seas. *Eos* **2015**, *96*. [CrossRef]

18. Stienessen, S.; McCarthy, A.; Jones, D.T.; Honkalehto, T. Results of the acoustic-trawl surveys of walleye pollock (*Gadus chalcogrammus*) in the Gulf of Alaska, February-March 2016 (DY2016-02 and DY2016-04). AFSC Processed Report 2017-02, 2017, Alaska Fisheries Science Center, NOAA, National Marine Fisheries Service, 7600 Sand Point Way NE, Seattle WA 98115. Available online: http://www.afsc.noaa.gov/Publications/ProcRpt/PR2017-02.pdf (accessed on 21 September 2019).

19. Kendall, A.W.; Piquelle, S.J. Egg and larval distributions of walleye pollock *Theragra chalcogramma* in Shelikof Strait, Gulf of Alaska. *Fish. Bull. USA* **1989**, *88*, 133–154.

20. Schumacher, J.D.; Kendall, A.W. Some interactions between young walleye pollock and their environment in the wester Gulf of Alaska. *CalCOFI Rep.* **1991**, *32*, 22–40.

21. Courtney, D.L.; Sigler, M.F. Trends in area-weighted CPUE of Pacific sleeper sharks *Somniosus pacificus* in the northeast Pacific Ocean determined from sablefish longline surveys. *Alaska Fish. Res. Bull.* **2007**, *12*, 292–316.

22. Laman, E.A.; Rooper, C.N.; Turner, K.; Rooney, S.; Cooper, D.; Zimmermann, M. Using species distribution models to define essential fish habitat in Alaska. *Can. J. Fish. Aquat. Sci.* **2017**, *75*, 1230–1255. [CrossRef]

23. Rooney, S.; Rooper, C.N.; Laman, E.A.; Turner, K.; Cooper, D.; Zimmermann, M. *Model-Based Essential Fish Habitat Definitions for Gulf of Alaska Groundfish Species*; U.S. Department Commerce: Washington, DC, USA, 2018.

24. Turner, K.; Rooper, C.N.; Laman, E.A.; Rooney, S.C.; Cooper, D.W.; Zimmermann, M. *Model-Based Essential Fish Habitat Definitions for Aleutian Island Groundfish Species*; U.S. Department Commerce: Washington, DC, USA, 2017.

25. Laman, E.A.; Rooper, C.N.; Rooney, S.C.; Turner, K.A.; Cooper, D.W.; Zimmermann, M. *Model-Based Essential Fish Habitat Definitions for Bering Sea Groundfish Species*; U.S. Department Commerce: Washington, DC, USA, 2017.

26. Zimmermann, M.; Reid, J.A.; Golden, N. Using smooth sheets to describe groundfish habitat in Alaskan waters. *Deep Sea Res. II Top. Stud. Oceanogr.* **2016**, *132*, 210–226. [CrossRef]

27. Zimmermann, M. Comparison of the physical attributes of the central and eastern Gulf of Alaska IERP inshore study sites. *Deep Sea Res. II Top. Stud. Oceanogr.* **2019**, *165*, 280–291. [CrossRef]

28. Zimmermann, M.; De Robertis, A.; Ormseth, O. Verification of historical smooth sheet bathymetry. *Deep Sea Res. II Top. Stud. Oceanogr.* **2019**, *165*, 292–302. [CrossRef]

29. Pirtle, J.; Shotwell, S.K.; Zimmermann, M.; Reid, J.A.; Golden, N. Habitat Suitability Models for Groundfish in the Gulf of Alaska. *Deep Sea Res. II Top. Stud. Oceanogr.* **2019**, *165*, 303–321. [CrossRef]

30. McGowan, D.W.; Horne, J.K.; Thorson, J.T.; Zimmermann, M. Influence of environmental factors on capelin distributions in the Gulf of Alaska. *Deep Sea Res. II Top. Stud. Oceanogr.* **2019**, *165*, 238–254. [CrossRef]

31. Mordy, C.W.; Stabeno, P.J.; Kachel, N.B.; Kachel, D.; Ladd, C.; Zimmermann, M.; Doyle, M. Importance of canyons to the northern gulf of Alaska ecosystem. *Deep Sea Res. II Top. Stud. Oceanogr.* **2019**, *165*, 203–220. [CrossRef]

32. Zimmermann, M.; Ruggerone, G.T.; Freymueller, J.T.; Kinsman, N.; Ward, D.H.; Hogrefe, K. Volcanic ash deposition, eelgrass beds, and inshore habitat loss from the 1920s to the 1990s at Chignik, Alaska. *Estuar. Coast. Shelf Sci.* **2018**, *202*, 69–86. [CrossRef]

33. Rooper, C.N.; Zimmermann, M.; Prescott, M.M.; Hermann, A.J. Predictive models of coral and sponge distribution, abundance and diversity in bottom trawl surveys of the Aleutian Islands, Alaska. *Mar. Ecol. Prog. Ser.* **2014**, *503*, 157–176. [CrossRef]

34. Rooper, C.N.; Zimmermann, M.; Prescott, M.M. Comparison of modeling methods to predict the spatial distribution of deep-sea coral and sponge in the Gulf of Alaska. *Deep Sea Res. Part I Oceanogr. Res. Pap.* **2017**, *126*, 148–161. [CrossRef]

35. Plafker, G.; Moore, J.C.; Winkler, G.R. *Geology of the Southern Alaska Margin*; Plafker, G., Berg, H.C., Eds.; Geological Society of America: Boulder, CO, USA, 1994; Volume G-1, pp. 389–449.

36. Coulter, H.W.; Hopkins, D.M.; Karlstrom, T.N.V.; Péwé, T.L.; Wahrhaftig, C.; Williams, J.R. *Map Showing Extent of glaciations in Alaska*; U.S. Geological Survey Miscellaneous Geologic Investigations Map, I-415; U.S. Geological Survey: Reston, VA, USA, 1965.

37. Hamilton, T.D. *Late Cenozoic Glaciation of Alaska*; Plafker, G., Berg, H.C., Eds.; Geological Society of America: Boulder, CO, USA, 1994; Volume G-1, pp. 813–844.

38. Kaufman, D.S.; Manley, W.F. Pleistocene Maximum and Late Wisconsinan glacier extents across Alaska, USA. In *Quaternary Glaciations—Extent and Chronology, Part II: North America. Developments in Quaternary Science*; Ehlers, J., Gibbard, P.L., Eds.; Elsevier: Amsterdam, The Netherlands, 2004; Volume 2B, pp. 9–27.

39. Misarti, N.; Finney, B.P.; Jordan, J.W.; Maschner, H.D.G.; Addison, J.A.; Shapley, M.D.; Krumhardt, A.; Beget, J.E. Early retreat of the Alaska Peninsula Glacier Complex and the implications for coastal migrations of first Americans. *Quat. Sci. Rev.* **2012**, *48*, 1–6. [CrossRef]

40. Mann, D.H.; Peteet, D.M. Extent and timing of the last glacial maximum in southwest Alaska. *Quat. Res.* **1994**, *42*, 136–148. [CrossRef]

41. Briner, J.P.; Tulenko, J.P.; Kaufman, D.S.; Young, N.E.; Baichtal, J.F.; Lesnek, A. The last deglaciation of Alaska. *Cuad. Investig. Geogr.* **2017**, *43*, 429–448. [CrossRef]

42. Detterman, R.L.; Miller, T.P.; Yount, M.E.; Wilson, F.H. *Quaternary Geologic Map of the Chignik and Sutwik Island Quadrangles, Alaska*; U.S. Geological Survey Miscellaneous Investigation Series Map I-1229, scale: 1:250,000, 1 sheet; U.S. Geological Survey: Reston, VA, USA, 1981.

43. Detterman, R.L.; Wilson, F.H.; Young, M.E.; Miller, T.P. *Quaternary Geologic Map of the Ugashik, Bristol Bay, and Western Part of Karluk Quadrangles, Alaska*; U.S. Geological Survey Miscellaneous Investigation Series Map I-1801, scale: 1:250,000; U.S. Geological Survey: Reston, VA, USA, 1987.

44. Wilson, F.H.; Detterman, R.L.; Miller, J.W.; Case, J.E. *Geologic Map of the Port Moller, Stepovak Bay, and Simeonof Island Quadrangles, Alaska Peninsula, Alaska*; U.S. Geological Survey Miscellaneous Investigation Series Map I-2272, scale: 1:250,000, 2 sheets; U.S. Geological Survey: Reston, VA, USA, 1995.

45. Wilson, F.H.; Weber, F.R.; Dochat, T.M.; Miller, T.P.; Detterman, R.L. *Revised Geologic Map of the Cold Bay and False Pass Quadrangles, Alaska Peninsula*; U.S. Geological Survey Open-File Report 97-866, scale: 1:250,000, 1 sheet; U.S. Geological Survey: Reston, VA, USA, 1997.

46. Kaufman, D.S.; Young, N.E.; Briner, J.P.; Manley, W.F. Alaska palaeo-glacier atlas (version 2). *Dev. Quat. Sci.* **2011**, *15*, 427–445. [CrossRef]

47. Clark, P.U.; Dyke, A.S.; Shakun, J.D.; Carlson, A.E.; Clark, J.; Wohlfarth, B.; Mitrovica, J.X.; Hostetler, S.W.; McCabe, A.M. The last glacial maximum. *Science* **2009**, *325*, 710–714. [CrossRef]

48. Prescott, M.M.; Zimmermann, M. *Smooth Sheet Bathymetry of Norton Sound*; U.S. Department Commerce: Washington, DC, USA, 2015.

49. Barry, C.; Legeer, S.; Parker, G.; VanSant, K.U.S. Office of Coast Survey's Re-Engineered Process for Application of Hydrographic Survey Data to NOAA Charts. 2005. Available online: http://www.nauticalcharts.noaa.gov/hsd/docs/SW_techpaper_barry.pdf (accessed on 21 September 2019).

50. Zimmermann, M.; Benson, J. *Smooth Sheets: How to Work with Them in a GIS to Derive Bathymetry, Features and Substrates*; U.S. Department Commerce: Washington, DC, USA, 2013.

51. Hampton, M.A. Quaternary sedimentation in Shelikof Strait, Alaska. *Mar. Geol.* **1985**, *62*, 213–253. [CrossRef]

52. Von Huene, R.; Hampton, M.A.; Fisher, M.A.; Varchol, D.J.; Cochrane, G.R. *Map Showing Near-Surface Geologic Structures of Kodiak Shelf, Alaska*; U.S. Geological Survey Miscellaneous Field Studies Map 1200, 1 sheet, scale: 1:500,000; U.S. Geological Survey: Reston, VA, USA, 1980.

53. Carver, G.; Sauber, J.; Lettis, W.; Witter, R.; Whitney, B.; Freymueller, J.T. Active faults on northeastern Kodiak Island, Alaska. *Act. Tecton. Seism. Potential Alask. Am. Geophys. Union Geophys. Monogr.* **2008**, *179*, 167–184.

54. Ramos, M.D. Earthquake Segment Boundaries and Tsunamigenic Faults of the Kodiak Segment, Alaska-Aleutian Subduction Zone. Master's Thesis, Boise State University, Boise, ID, USA, 2017.

55. Berndt, C. Focused fluid flow in passive continental margins. *Philos. Trans. R. Soc. A* **2005**, *363*, 2855–2871. [CrossRef]

56. Judd, A.G.; Hovland, M. *Seabed Fluid Flow: The Impact of Geology, Biology and the Marine Environment*; Cambridge University Press: Cambridge, UK, 2007; Volume 15, p. 475.

57. Newman, K.R.; Cormier, M.H.; Weissel, J.K.; Driscoll, N.W.; Kastner, M.; Solomon, E.A.; Robertson, G.; Hill, J.C.; Singh, H.; Camilli, R.; et al. Active methane venting observed at giant pockmarks along the US mid-Atlantic shelf break. *Earth Planet. Sci. Lett.* **2008**, *267*, 341–352. [CrossRef]

58. Bøe, R.; Rise, L.; Ottesen, D. Elongate depressions on the southern slope of the Norwegian Trench (Skagerrak): Morphology and evolution. *Mar. Geol.* **1998**, *146*, 191–203. [CrossRef]

59. Dowdeswell, J.A.; Canals, M.; Jakobsson, M.; Todd, B.J.; Dowdeswell, E.K.; Hogan, K. (Eds.) *Atlas of Submarine Glacial Landforms: Modern, Quaternary and Ancient*; Geological Society of London: London, UK, 2016; p. 618.

60. Ottesen, D.; Dowdeswell, J.A. Assemblages of submarine landforms produced by tidewater glaciers in Svalbard. *J. Geophys. Res. Earth Surf.* **2006**, *111*. [CrossRef]

61. Ottesen, D.; Dowdeswell, J.A.; Benn, D.I.; Kristensen, L.; Christiansen, H.H.; Christensen, O.; Hansen, L.; Lebesbye, E.; Forwick, M.; Vorren, T.O. Submarine landforms characteristic of glacier surges in two Spitsbergen fjords. *Quat. Sci. Rev.* **2008**, *27*, 1583–1599. [CrossRef]

62. Brown, C.S.; Newton, A.M.; Huuse, M.; Buckley, F. Iceberg scours, pits, and pockmarks in the North Falkland Basin. *Mar. Geol.* **2017**, *386*, 140–152. [CrossRef]

63. López-Martínez, J.; Muñoz, A.; Dowdeswell, J.A.; Linés, C.; Acosta, J. Relict sea-floor ploughmarks record deep-keeled Antarctic icebergs to 45 S on the Argentine margin. *Mar. Geol.* **2011**, *288*, 43–48. [CrossRef]

64. Syvitski, J.P.M.; Stein, A.B.; Andrews, J.T.; Milliman, J.D. Icebergs and the sea floor of the East Greenland (Kangerlussuaq) continental margin. *Arct. Antarct. Alp. Res.* **2001**, *33*, 52. [CrossRef]

65. Fairbanks, R.G. A 17,000-year glacio-eustatic sea level record: Influence of glacial melting rates on the Younger Dryas event and deep-ocean circulation. *Nature* **1989**, *342*, 637–642. [CrossRef]

66. Food and Agriculture Organization. The state of world fisheries and aquaculture 2016. In *Contributing to Food Security and Nutrition for All*; FAO: Rome, Italy, 2016.

67. Schumacher, J.D.; Stabeno, P.J.; Roach, A.T. Volume transport in the Alaska Coastal Current. *Cont. Shel. Res.* **1989**, *9*, 1071–1083. [CrossRef]

68. Reed, R.K.; Schumacher, J.D.; Incze, L.S. Circulation in Shelikof Strait, Alaska. *J. Phys. Oceanogr.* **1987**, *17*, 1546–1554. [CrossRef]

69. Bograd, S.J.; Stabeno, P.J.; Schumacher, J.D. A census of mesoscale eddies in Shelikof Strait. *J. Geophys. Res.* **1994**, *99*, 18243–18254. [CrossRef]

70. Schumacher, J.D.; Stabeno, P.J.; Bograd, S.J. Characteristics of an eddy over a continental shelf: Shelikof Strait, Alaska. *J. Geophys. Res.* **1993**, *98*, 8395–8404. [CrossRef]

71. Bacheler, N.M.; Bailey, K.M.; Ciannelli, L.; Bartolino, V.; Chan, K.S. Density-dependent, landscape, and climate effects on spawning distribution of walleye pollock *Theragra chalcogramma*. *Mar. Ecol. Prog. Ser.* **2009**, *391*, 1–12. [CrossRef]

72. Schumacher, J.D.; Reed, R.K. Coastal flow in the northwest Gulf of Alaska: The Kenai current. *J. Geophys. Res.* **1980**, *85*, 6680–6688. [CrossRef]

73. Hart, J.L. *Pacific Fishes of Canada*; Bulletin 180; Fisheries Research Board of Canada: Ottawa, ON, Canada, 1975.

74. Tribuzio, C.A.; Hulson, P.-J.; Echave, K.; Rodgveller, C. Assessment of the shark stock complex in the Gulf of Alaska. In *Stock Assessment and Fishery Evaluation Report for the Groundfish Resources of the Gulf of Alaska*; North Pacific Fishery Management Council: Anchorage, AK, USA, 2017; pp. 1343–1346.

75. Mayer, L.; Jakobsson, M.; Allen, G.; Dorschel, B.; Falconer, R.; Ferrini, V.; Lamarche, G.; Snaith, H.; Weatherall, P. The Nippon Foundation—GEBCO seabed 2030 project: The quest to see the world's oceans completely mapped by 2030. *Geosciences* **2018**, *8*, 63. [CrossRef]

76. NOAA. 2-minute Gridded Global Relief Data (ETOPO2) v2. 2006. Available online: https://data.nodc.noaa.gov/cgi-bin/iso?id=gov.noaa.ngdc.mgg.dem:301 (accessed on 10 April 2018).

77. Brothers, D.S.; Haeussler, P.; East, A.; ten Brink, U.; Andrews, B.; Dartnell, P.; Miller, N.; Kluesner, J. A closer look at an undersea source of Alaskan earthquakes. *EOS* **2018**, *99*, 22–26. [CrossRef]

78. Batchelor, C.L.; Dowdeswell, J.A. The physiography of high Arctic cross-shelf troughs. *Quat. Sci. Rev.* **2014**, *92*, 68–96. [CrossRef]

79. Karlstrom, T.N.V. Upper Cook Inlet region, Alaska, in Multiple Glaciation in Alaska: U.S. *Geol. Surv. Circ.* **1953**, *289*, 1–13.

80. Hajdas, I.; Bonani, G.; Bodén, P.; Peteet, D.M.; Mann, D.H. Cold reversal on Kodiak Island, Alaska, correlated with the European Younger Dryas by using variations of atmospheric 14C content. *Geology* **1998**, *26*, 1047–1050. [CrossRef]

81. Briner, J.P.; Kaufman, D.S.; Werner, A.; Caffee, M.; Levy, L.; Manley, W.F.; Kaplan, M.R.; Finkel, R.C. Glacier readvance during the late glacial (Younger Dryas?) in the Ahklun Mountains, southwestern Alaska. *Geology* **2002**, *30*, 679–682. [CrossRef]